Ehrlich occupancy time: Beyond k_{off} to a complete residence time framework

Justin Eilertsen
Mathematical Reviews
American Mathematical Society
416 4th Street
Ann Arbor, MI, 48103
e-mail: jse@ams.org

Santiago Schnell
Department of Mathematics
Dartmouth, Hanover, NH 03755
Department of Biochemistry & Cell Biology, and
Department of Biomedical Data Sciences
Geisel School of Medicine at Dartmouth, Hanover, NH 03755
e-mail: santiago.schnell@dartmouth.edu

Sebastian Walcher
Fachgruppe Mathematik, RWTH Aachen
D-52056 Aachen, Germany
e-mail: walcher@mathga.rwth-aachen.de

December 10, 2025

Abstract

Drug-target occupancy time—the cumulative duration a target remains bound—critically influences therapeutic efficacy. While Copeland's widely-used residence time ($1/k_{\text{off}}$) emphasizes dissociation kinetics, it neglects association rates, rebinding events, and drug elimination that affect in vivo outcomes. Returning to Paul Ehrlich's 1913 principle that drugs act only when bound ("Corpora non agunt nisi fixata"), we develop a mathematically rigorous framework defining Ehrlich occupancy time as the integral of fractional target occupancy over time. Our approach explicitly incorporates association (k_{on}) and dissociation (k_{off}) kinetics, accounts for rebinding, and extends to systems with drug removal. For drug-receptor closed systems at equilibrium, we prove that relative Ehrlich occupancy time equals $b_0/(K_d+b_0)$, where K_d is the dissociation constant and b_0 the drug concentration. For induced-fit mechanisms, conformational changes reduce the effective dissociation constant to $K_d^* = K_d/(1 + k_3/k_4)$ (where k_3 and k_4 are forward and reverse isomerization rates), prolonging occupancy through kinetic trapping. Critically, for drug-receptor systems with first-order drug elimination at rate k_3, we derive rigorous bounds:

$b_0/[(b_0 + K_d)k_3] \leq \mathrm{EOT}_\infty \leq b_0/(K_d \cdot k_3)$, revealing that both binding affinity and elimination rate jointly determine occupancy. This explains why high-affinity drugs can fail clinically if eliminated rapidly, and identifies pharmacokinetic optimization opportunities. We prove Copeland's definition is a special case of Ehrlich occupancy time when rebinding is absent. Our framework provides quantitative tools for optimizing drug design beyond binding affinity and enables improved prediction of in vivo efficacy where pharmacokinetics dominate.

Keywords: drug-target kinetics, residence time, pharmacokinetics, receptor occupancy, mass action kinetics, binding kinetics

1 Introduction

The development of effective therapeutics requires understanding not merely how strongly drugs bind to their targets, but how long they remain bound. Traditional drug discovery has emphasized binding affinity—quantified by the equilibrium dissociation constant K_d—as the primary metric for drug-target interactions. However, binding affinity alone often fails to predict therapeutic efficacy [1, 2]. Drugs with moderate affinity may exhibit prolonged effects due to extended binding durations, while high-affinity compounds can dissociate rapidly, yielding short-lived responses [3, 4].

The insight that the *duration* of drug-target binding critically determines drug efficacy traces to Paul Ehrlich's 1913 principle [5]: "Corpora non agunt nisi fixata" –substances act only when bound. Ehrlich recognized that therapeutic effect depends on the cumulative time a target remains occupied by drug molecules. Building on this foundation, Copeland and colleagues introduced "drug-target residence time" (DTRT), defined as the reciprocal of the dissociation rate constant: $\mathrm{DTRT} = 1/k_{\mathrm{off}}$ [1, 6, 7]. This concept has influenced modern drug design, particularly for kinase inhibitors [8] and antibiotics [9, 10], where prolonged target engagement correlates with enhanced efficacy.

However, Copeland's DTRT definition has significant limitations. First, it considers only dissociation kinetics, neglecting the association rate (k_{on}) and thereby ignoring how quickly drugs initially engage targets. Second, it excludes rebinding events—when dissociated drug molecules reassociate with the same or nearby targets—which can substantially extend effective target occupancy in vivo [11]. Third, DTRT assumes equilibrium conditions and does not account for drug removal processes (metabolism, excretion) that dominate in physiological settings. Folmer [12] critiqued DTRT as "misleading," noting that its predictive value often reduces merely to potency and that claims of benefits beyond drug clearance lack robust experimental support.

While our framework is general and applicable to diverse drug-target binding scenarios, we demonstrate its utility through three clinically relevant exemplary cases: (i) simple receptor-ligand binding in closed systems, (ii) induced-fit mechanisms with conformational changes, and (iii) systems with first-order drug removal. These examples span the range from idealized biochemical assays to physiologically relevant in vivo conditions.

We return to Ehrlich's original concept to develop a mathematically rigorous framework for what we term **Ehrlich occupancy time (EOT)**—the total cumulative duration that target molecules are occupied by drug, explicitly including rebinding events and drug removal. Our approach defines EOT rigorously through chemical kinetics, incorporating both k_{on} and k_{off}; quantifies EOT in closed systems, showing that relative EOT equals the equilibrium fraction of bound receptors and that K_d is the appropriate metric; derives analytical bounds for EOT in systems with first-order drug removal, revealing how pharmacokinetic parameters constrain therapeutic duration; extends the framework to induced-fit mechanisms; and proves that EOT reduces to Copeland's DTRT only in the absence of rebinding.

Our framework addresses key questions: How do association and dissociation kinetics jointly determine occupancy time? When does drug removal limit therapeutic duration? How do conformational changes in the target affect residence time? The answers provide quantitative guidance for drug design and more accurate prediction of in vivo efficacy.

For context, we note related literature: Copeland's residence time applies well to cases like kinase inhibitors [8], but in complex systems, rebinding and pharmacokinetics necessitate broader views [11]. Our framework integrates kinetics holistically. Detailed derivations are in appendices, with main text focusing on implications.

This paper is organized as follows. Section 2 develops the mathematical definition of EOT. Section 3 applies the framework to closed systems (receptor-ligand binding, induced fit). Section 4 analyzes systems with drug removal, deriving computable bounds. Section 5 discusses implications for drug discovery. Our framework integrates kinetics holistically, with detailed derivations provided in the appendices and the main text focusing on implications.

2 Mathematical Definition of Ehrlich Occupancy Time

2.1 Conceptual Foundation and Discrete-Time Formulation

Consider a population of target receptors interacting with drug molecules over an observation period $[0, T]$. At any time t, each receptor is either free (unoccupied) or bound (occupied by a drug molecule). The **Ehrlich occupancy time (EOT)** is the average cumulative duration that receptors spend in the bound state during $[0, T]$.

To understand this concept, consider the schematic representation in Figure 1. For a given receptor, we track whether it is occupied (shaded regions) or free (unshaded regions) throughout the observation period.

Ehrlich occupancy time (EOT): Sum the durations of *all* time intervals when the receptor is occupied, including multiple binding events. For Receptor 1 in Figure 1C, if the receptor is occupied during three separate periods, EOT includes all three. Averaging over all receptors gives the mean EOT for the system.

Copeland residence time: Measure only the duration of the *first* binding event, from initial association to first dissociation, ignoring any subsequent rebinding. For Receptor 2 in Figure 1D, which undergoes multiple binding/unbinding cycles, Copeland residence time counts only the first shaded region. This provides the mean "dwell time" per binding event but misses cumulative target engagement.

The key distinction is that **EOT captures total target occupancy** (relevant to Ehrlich's principle that drugs act only when bound), while **Copeland residence time captures single-event kinetics** (relevant when rebinding is negligible). As we show in Section 3, Copeland residence time equals EOT only in the special case where no rebinding occurs.

2.1.1 Formal Construction

We now formalize these concepts mathematically. Consider a finite set of receptors

$$\mathcal{R} := \{R_1, \ldots, R_N\},$$

where each receptor R_i can be in one of two states at any time $t \geq 0$: occupied (bound by a ligand) or free (unoccupied). We observe the system over the interval $[0, T]$, which we partition into M discrete time points:

$$0 = t_0 < t_1 < \cdots < t_M = T,$$

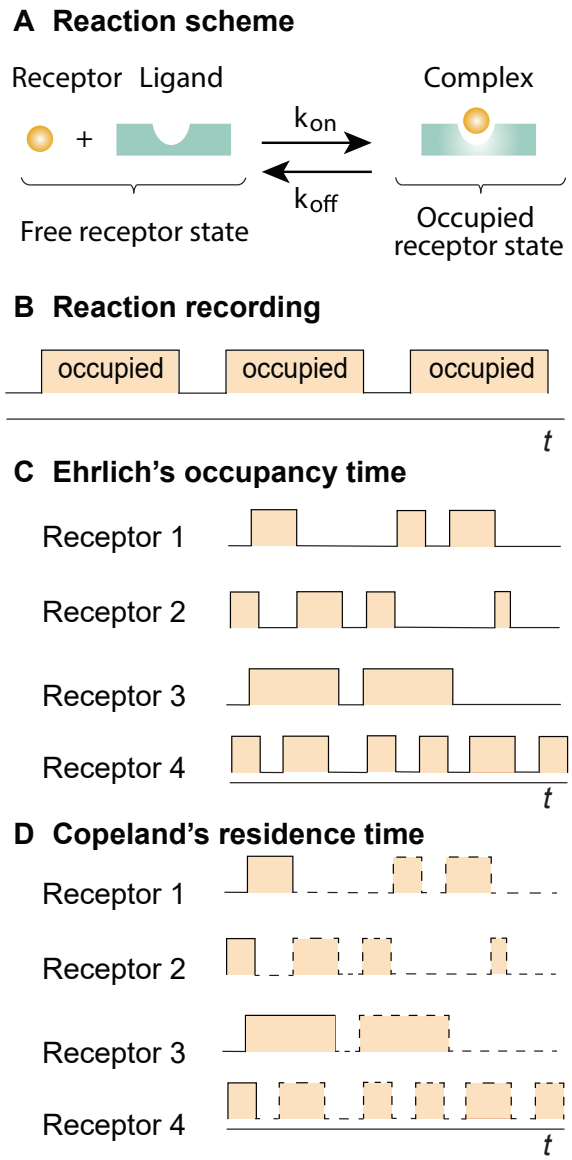

Figure 1: **Conceptual comparison of Ehrlich occupancy time (EOT) and Copeland residence time. (A)** Schematic of drug-target binding reaction showing reversible association with rate constant k_{on} and dissociation with rate constant k_{off}. **(B)** Reaction scheme indicating transitions between free receptor state (left) and occupied receptor state (right, with bound complex shown). **(C)** Ehrlich occupancy time (EOT) calculation: For each receptor (rows 1–4), occupied periods are shown as shaded regions along the time axis. EOT for a single receptor is the sum of *all* occupied intervals, including rebinding events. For example, Receptor 2 experiences four separate binding events; all four contribute to its EOT. The average EOT across all receptors is the arithmetic mean of individual EOT values. **(D)** Copeland residence time calculation: For each receptor, only the duration of the *first* binding event is counted (solid shaded regions), from initial association to first dissociation. Subsequent rebinding events (dashed outlines) are excluded from the calculation. For Receptor 2, only the first binding period contributes to Copeland residence time, despite multiple occupancy events. The average Copeland residence time is the arithmetic mean of first-binding durations. **Key distinction:** EOT measures cumulative target occupancy (total time bound), reflecting Ehrlich's principle that drugs act when fixed to targets. Copeland residence time measures single-event kinetics, equaling $1/k_{\text{off}}$. The two metrics coincide only when no rebinding occurs (see Appendix 2.4).

with uniform spacing $\Delta t = t_{j+1} - t_j = T/M$ for all $j = 0, 1, \ldots, M-1$.

The occupancy status of each receptor at each observation time is captured by the indicator function:

$$\mathrm{OS}(R_i, t_j) = \begin{cases} 1, & \text{if receptor } R_i \text{ is occupied at time } t_j \\ 0, & \text{otherwise.} \end{cases} \tag{1}$$

For an individual receptor R_i, assuming the occupancy status remains constant within each interval $(t_{j-1}, t_j]$, the total time spent in the occupied state is approximated by:

$$\mathrm{OT}(R_i) := \Delta t \cdot \sum_{j=1}^{M} \mathrm{OS}(R_i, t_j). \tag{2}$$

At each time point t_j, the number of occupied receptors is

$$\mathrm{NO}(t_j) := \sum_{i=1}^{N} \mathrm{OS}(R_i, t_j), \tag{3}$$

and the fraction of occupied receptors is

$$f(t_j) := \frac{\mathrm{NO}(t_j)}{N}. \tag{4}$$

The **Ehrlich occupancy time** is defined as the average occupancy time across all receptors:

$$\begin{aligned} \mathrm{EOT} &= \frac{1}{N} \sum_{i=1}^{N} \mathrm{OT}(R_i) \\ &= \frac{1}{N} \sum_{i=1}^{N} \left(\Delta t \cdot \sum_{j=1}^{M} \mathrm{OS}(R_i, t_j) \right) \\ &= \frac{\Delta t}{N} \sum_{j=1}^{M} \sum_{i=1}^{N} \mathrm{OS}(R_i, t_j) \quad \text{(exchanging order of summation)} \\ &= \Delta t \sum_{j=1}^{M} \frac{\mathrm{NO}(t_j)}{N} \\ &= \sum_{j=1}^{M} f(t_j) \cdot \Delta t. \end{aligned} \tag{5}$$

Equation (5) expresses the discrete-time EOT as a weighted sum of the fractional occupancy at each observation time. This formulation has an important consequence: *EOT can be computed from the population-level quantity $f(t_j)$ without tracking individual receptors.* This connects the microscopic definition (averaging over individual receptor trajectories) to the macroscopic observable (fraction of receptors bound at each time).

Example 1 (Discrete-Time Illustration)**.** *Consider $N = 3$ receptors observed at $M = 4$ time points over period $T = 4$ time units, so $\Delta t = 1$. Suppose the occupancy status is recorded as:*

Receptor	t_1	t_2	t_3	t_4	$\mathrm{OT}(R_i)$
R_1	*1*	*1*	*0*	*0*	*2*
R_2	*1*	*1*	*1*	*0*	*3*
R_3	*0*	*1*	*1*	*1*	*3*
$\mathrm{NO}(t_j)$	*2*	*3*	*2*	*1*	
$f(t_j)$	$\frac{2}{3}$	1	$\frac{2}{3}$	$\frac{1}{3}$	

The EOT can be computed either by averaging individual receptor occupancy times,

$$\mathrm{EOT} = \frac{1}{3}(2+3+3) = \frac{8}{3} \approx 2.67 \text{ time units},$$

or equivalently, by summing the fractional occupancies,

$$\mathrm{EOT} = \Delta t \sum_{j=1}^{4} f(t_j) = 1 \cdot \left(\frac{2}{3} + 1 + \frac{2}{3} + \frac{1}{3}\right) = \frac{8}{3} \text{ time units.}$$

Both approaches yield the same result, confirming the equivalence established in equation (5).

Remark 1 (Dependence on Δt)**.** *The discrete-time formulation* (5) *depends on the choice of time step* Δt*. For a fixed observation period* T*, finer temporal resolution (smaller* Δt*, larger* M*) generally provides a more accurate approximation of the true cumulative occupancy. In the next subsection, we take the limit* $\Delta t \to 0$ *to obtain the continuous-time formulation, which eliminates this dependence.*

2.2 Continuous-Time Formulation

The discrete-time EOT in equation (5) depends on the choice of partition, and should be viewed as an approximation whose accuracy improves as Δt decreases. To obtain a formulation independent of the observation frequency, we pass to the continuous-time limit.

2.2.1 From Discrete to Continuous Time

Consider the general setting of free receptors (X_i), bound complexes (Y_j), and other species including ligands (Z_k). The concentrations of these species evolve according to a system of ordinary differential equations derived from the reaction kinetics.[1] The fraction of occupied receptors at any time t is given by:

$$f(t) := \frac{\sum_j y_j(t)}{\sum_i x_i(t) + \sum_j y_j(t)}, \tag{6}$$

where lowercase letters denote concentrations. In closed systems, the total receptor concentration $\sum_i x_i + \sum_j y_j$ is conserved, so the denominator remains constant.

Recall from equation (5) that the discrete-time EOT is given by:

$$\mathrm{EOT} = \sum_{j=1}^{M} f(t_j) \cdot \Delta t = \sum_{j=1}^{M} f(t_j) \cdot (t_j - t_{j-1}).$$

[1] In the present paper, the right-hand sides are polynomial, derived from mass action kinetics, but the approach applies to more general kinetics as well.

This expression is a *Riemann sum* for the function f over the interval $[0, T]$, where the time points $t_0 < t_1 < \cdots < t_M$ form a partition with uniform subinterval length $\Delta t = T/M$.

A fundamental result in analysis [13] states that if $f : [0, T] \to \mathbb{R}$ is continuous, then the Riemann sum converges to the definite integral as the partition is refined:

$$\lim_{\Delta t \to 0} \sum_{j=1}^{M} f(t_j) \cdot (t_j - t_{j-1}) = \int_0^T f(t)\,\mathrm{d}t. \tag{7}$$

Equivalently, taking $M \to \infty$ while holding T fixed (so that $\Delta t = T/M \to 0$) yields the same limit.

When the concentrations $x_i(t)$ and $y_j(t)$ are governed by systems of ordinary differential equations with continuous right-hand sides, the solutions are continuous functions of time, and hence $f(t)$ as defined in (6) is continuous on $[0, T]$. The convergence (7) therefore applies, justifying the following definition.

Definition 1 (Ehrlich Occupancy Time)**.** *The **Ehrlich occupancy time** over the interval $[0, T]$ is defined as:*

$$\boxed{\mathrm{EOT}(T) := \int_0^T f(t)\,\mathrm{d}t} \tag{8}$$

where $f(t)$ is the fraction of receptors occupied at time t.

Equation (8) is our primary definition and serves as the foundation for all subsequent analysis. It has a natural interpretation: $\mathrm{EOT}(T)$ is the area under the fractional occupancy curve from time 0 to time T. The discrete-time formulation (5) provides an approximation to this integral, with accuracy improving as $\Delta t \to 0$.

2.2.2 Connection to Experimental Measurements

While equation (8) is defined theoretically, it connects directly to experimentally measurable quantities. The fraction $f(t)$ can be determined experimentally using several complementary techniques. Surface plasmon resonance (SPR) provides real-time measurement of bound complex concentration, yielding $f(t)$ directly when the response is normalized by total binding capacity. Radioligand binding assays measure bound radioactivity at multiple time points to construct $f(t)$ profiles. For live-cell applications, fluorescence-based target engagement assays using FRET or fluorescence polarization can monitor the bound fraction in real time. Cellular thermal shift assays (CETSA) offer an alternative approach, indirectly reporting target occupancy through the stabilization of target proteins against thermal denaturation.

Experimental determination of EOT thus requires measuring $f(t)$ at multiple time points over the observation period $[0, T]$ and numerically integrating. The discrete-time formula (5) corresponds to a left-endpoint Riemann sum; in practice, the trapezoidal rule or Simpson's rule may provide better accuracy for a given number of measurements. Alternatively, if binding kinetics are well-characterized (known rate constants), one can predict $f(t)$ computationally and calculate EOT analytically or numerically. Detailed experimental protocols for measuring kinetic parameters and validating EOT predictions are provided in Appendix B.

In Sections 3–4, we evaluate the integral in (8) for specific binding mechanisms to obtain closed-form expressions or computable bounds for EOT.

2.3 Relative Ehrlich Occupancy Time

For closed systems approaching equilibrium, the fractional occupancy $f(t)$ converges to a limiting value f_∞ as $t \to \infty$. In this setting, $\mathrm{EOT}(T)$ grows without bound as T increases, making it useful to consider a normalized quantity.

Definition 2 (Relative Ehrlich Occupancy Time)**.** *The* ***relative Ehrlich occupancy time*** *over the interval* $[0, T]$ *is defined as:*

$$\mathrm{rEOT}(T) := \frac{\mathrm{EOT}(T)}{T} = \frac{1}{T}\int_0^T f(t)\,\mathrm{d}t. \tag{9}$$

The relative EOT represents the time-averaged fractional occupancy over $[0, T]$. The following proposition establishes that, for systems approaching equilibrium, this average converges to the equilibrium occupancy.

Proposition 1. *Let* $f : [0, \infty) \to [0, 1]$ *be a continuous function satisfying* $f(t) \to f_\infty$ *as* $t \to \infty$ *for some* $f_\infty \in [0, 1]$*. Then*

$$\lim_{T\to\infty} \mathrm{rEOT}(T) = \lim_{T\to\infty} \frac{1}{T}\int_0^T f(t)\,\mathrm{d}t = f_\infty. \tag{10}$$

Proof. Since $0 \le f(t) \le 1$ for all $t \ge 0$, the function f is bounded. Let $\varepsilon > 0$ be arbitrary. Under the assumption that $f(t) \to f_\infty$, there exists $T_0 > 0$ such that $|f(t) - f_\infty| < \varepsilon$ for all $t \ge T_0$.

For any $T > T_0$, we decompose the integral:

$$\frac{1}{T}\int_0^T f(t)\,\mathrm{d}t - f_\infty = \frac{1}{T}\int_0^T [f(t) - f_\infty]\,\mathrm{d}t = \frac{1}{T}\int_0^{T_0} [f(t) - f_\infty]\,\mathrm{d}t + \frac{1}{T}\int_{T_0}^T [f(t) - f_\infty]\,\mathrm{d}t.$$

For the first integral, since $|f(t) - f_\infty| \le 1$ for all t:

$$\left|\frac{1}{T}\int_0^{T_0} [f(t) - f_\infty]\,\mathrm{d}t\right| \le \frac{T_0}{T}.$$

For the second integral, using $|f(t) - f_\infty| < \varepsilon$ for $t \ge T_0$:

$$\left|\frac{1}{T}\int_{T_0}^T [f(t) - f_\infty]\,\mathrm{d}t\right| \le \frac{1}{T}\int_{T_0}^T \varepsilon\,\mathrm{d}t = \varepsilon \cdot \frac{T - T_0}{T} < \varepsilon.$$

Combining these estimates:

$$\left|\frac{1}{T}\int_0^T f(t)\,\mathrm{d}t - f_\infty\right| < \frac{T_0}{T} + \varepsilon.$$

For all $T > T_0/\varepsilon$, we have $T_0/T < \varepsilon$, and therefore:

$$|\mathrm{rEOT}(T) - f_\infty| < 2\varepsilon.$$

Since $\varepsilon > 0$ was arbitrary, this establishes that $\mathrm{rEOT}(T) \to f_\infty$ as $T \to \infty$. □

Proposition 1 provides a direct connection between residence time and target occupancy: *for systems at equilibrium, the relative EOT equals the equilibrium fraction of bound receptors.* This result justifies the use of f_∞ as an approximation for $\mathrm{rEOT}(T)$ when T is sufficiently large and the system has equilibrated.

Remark 2 (Practical Implications)**.** *Relative EOT is particularly useful for comparing drugs in* in vitro *binding assays where the system reaches equilibrium. Since EOT(T) grows approximately linearly with time in equilibrated systems (EOT(T)* $\approx f_\infty \cdot T$ *for large T), the ratio EOT(T)/T provides a time-independent metric that depends only on the binding kinetics and drug concentration.*

In Section 3, we derive explicit expressions for f_∞ *(and hence rEOT) for several binding mechanisms. For systems with drug removal (Section 4), where equilibrium is never reached and* $f(t) \to 0$ *as* $t \to \infty$*, one must instead analyze the limiting value* $\mathrm{EOT}_\infty = \lim_{T\to\infty} \mathrm{EOT}(T)$*, which remains finite.*

2.4 Relationship to Copeland DTRT

A natural question is how our framework relates to Copeland's widely-used definition DTRT $= 1/k_{\text{off}}$ [1]. We now show that Copeland's metric emerges as a special limiting case of EOT when rebinding is absent.

2.4.1 Derivation of Copeland DTRT as a Limiting Case

Consider a scenario where rebinding is prevented—for example, by infinite dilution or rapid removal of dissociated ligand. This situation is modeled by irreversible dissociation:

$$\text{C} \xrightarrow{k_2} \text{A} + \text{B} \tag{11}$$

with no reverse (association) reaction, corresponding to $k_1 = 0$. Starting from an initial complex concentration $c(0) = c_0$, the complex decays according to first-order kinetics:

$$\dot{c} = -k_2 c, \qquad c(0) = c_0. \tag{12}$$

The solution is exponential decay:

$$c(t) = c_0 \exp(-k_2 t). \tag{13}$$

Taking the receptor concentration as $a_0 = c_0$ (all receptors initially bound), the fractional occupancy is $f(t) = c(t)/c_0 = \exp(-k_2 t)$. The total Ehrlich occupancy time is:

$$\begin{aligned} \text{EOT}(\infty) &= \int_0^\infty f(t)\,\mathrm{d}t \\ &= \int_0^\infty \exp(-k_2 t)\,\mathrm{d}t \\ &= \frac{1}{k_2}. \end{aligned} \tag{14}$$

This is precisely Copeland's definition: DTRT $= 1/k_{\text{off}}$, where $k_{\text{off}} = k_2$ is the dissociation rate constant.

2.4.2 Interpretation and Implications

This derivation has two important implications. First, it establishes that Copeland DTRT is a special case of EOT: when rebinding is absent ($k_1 = 0$), the Ehrlich occupancy time reduces exactly to the Copeland metric, demonstrating that our framework generalizes, rather than contradicts, the existing definition. Second, the derivation shows that rebinding extends occupancy time. In general binding scenarios (Section 3) where $k_1 > 0$, dissociated drug molecules can reassociate with receptors, contributing additional occupied time. Consequently, EOT exceeds Copeland DTRT, and the difference between EOT and $1/k_2$ quantifies the contribution of rebinding to cumulative target occupancy.

Referring to Figure 1, Copeland DTRT corresponds to measuring only the first shaded region for each receptor (panel D), while EOT measures all shaded regions (panel C). The two metrics coincide only when there is at most one shaded region per receptor—that is, when rebinding does not occur.

Remark 3 (When is Rebinding Negligible?)**.** *The Copeland limit ($k_1 = 0$) applies under specific conditions: when experiments are conducted under "infinite dilution" conditions where dissociated ligand is immediately*

removed or diluted below effective concentration; when the dissociation rate greatly exceeds the effective association rate ($k_2 \gg k_1 b(t)$) for all relevant times; or when drug elimination is much faster than rebinding ($k_3 \gg k_1 b(t)$), where k_3 is the elimination rate discussed in Section 4. In typical in vivo settings, none of these conditions hold, and rebinding contributes significantly to target occupancy. This is why EOT provides a more complete measure of therapeutic duration than DTRT.

3 Ehrlich Occupancy Time in Closed Systems

We first analyze closed systems (no influx or efflux of species), which model typical in vitro binding assays. These systems approach equilibrium as $t \to \infty$, allowing us to compute rEOT analytically via Proposition 1.

3.1 Fundamental Receptor-Ligand Binding

Consider the reversible bimolecular reaction:

$$\mathrm{A} + \mathrm{B} \underset{k_2}{\overset{k_1}{\rightleftharpoons}} \mathrm{C} \tag{15}$$

where A is the receptor (target), B is the drug (ligand), and C is the drug-receptor complex. Let $a(t)$, $b(t)$, and $c(t)$ denote the concentrations of these species at time t, with initial conditions $a(0) = a_0$, $b(0) = b_0$, and $c(0) = 0$ (no complex initially present).

Mass-action kinetics yields the system of ordinary differential equations:

$$\begin{aligned} \dot{a} &= -k_1 ab + k_2 c \\ \dot{b} &= -k_1 ab + k_2 c \\ \dot{c} &= k_1 ab - k_2 c \end{aligned} \tag{16}$$

where k_1 (units: $\mathrm{M}^{-1}\mathrm{s}^{-1}$) is the association rate constant and k_2 (units: s^{-1}) is the dissociation rate constant. The system satisfies two conservation laws:

$$a(t) + c(t) = a_0, \qquad b(t) + c(t) = b_0, \tag{17}$$

reflecting conservation of total receptor and total ligand, respectively. The fraction of occupied receptors at time t is $f(t) = c(t)/a_0$.

3.1.1 Equilibrium Analysis

At equilibrium, the forward and reverse reaction rates balance: $k_1 a_\infty b_\infty = k_2 c_\infty$. Using the conservation laws (17) to substitute $a_\infty = a_0 - c_\infty$ and $b_\infty = b_0 - c_\infty$, we obtain:

$$k_1(a_0 - c_\infty)(b_0 - c_\infty) = k_2 c_\infty. \tag{18}$$

Expanding and rearranging yields a quadratic equation in c_∞:

$$k_1 c_\infty^2 - [k_1(a_0 + b_0) + k_2]c_\infty + k_1 a_0 b_0 = 0. \tag{19}$$

Applying the quadratic formula and selecting the physically meaningful root (satisfying $0 \le c_\infty \le \min(a_0, b_0)$), we obtain after simplification:

$$c_\infty = \frac{a_0 + b_0 + K_d}{2}\left(1 - \sqrt{1 - \frac{4a_0 b_0}{(a_0 + b_0 + K_d)^2}}\right), \tag{20}$$

Table 1: Glossary of key terms and parameters.

Term/Symbol	**Definition**
EOT	Ehrlich Occupancy Time: cumulative duration target is occupied, including all binding/unbinding cycles
rEOT	Relative EOT: $\mathrm{EOT}(T)/T$, converges to equilibrium occupancy fraction
DTRT	Drug-Target Residence Time (Copeland): $1/k_{\mathrm{off}}$, duration of single binding event
k_1 (or k_{on})	Association rate constant ($\mathrm{M}^{-1}\mathrm{s}^{-1}$): how fast drug binds to free target
k_2 (or k_{off})	Dissociation rate constant (s^{-1}): how fast drug-target complex dissociates
k_3	Elimination rate constant (s^{-1}): how fast drug is removed from system
K_d	Dissociation constant (k_2/k_1, units M): lower K_d = tighter binding
$f(t)$	Fractional target occupancy at time t: fraction of targets bound by drug
a_0, b_0	Initial concentrations of target and drug, respectively
Rebinding	Drug molecule dissociates then reassociates before elimination
Induced fit	Conformational change in target upon drug binding (mechanism in equation (25))
Pseudo-first-order	Approximation valid when target concentration $\ll$ drug concentration

where $K_d = k_2/k_1$ is the **dissociation constant** (units: M). The equilibrium fraction of bound receptors is therefore:

$$f_\infty = \frac{c_\infty}{a_0} = \frac{a_0 + b_0 + K_d}{2a_0}\left(1 - \sqrt{1 - \frac{4a_0 b_0}{(a_0 + b_0 + K_d)^2}}\right). \tag{21}$$

By Proposition 1, this equals the limiting relative EOT: $\mathrm{rEOT}(T) \to f_\infty$ as $T \to \infty$.

3.1.2 Pseudo-First-Order Approximation

The exact expression (21) is difficult to interpret. Considerable simplification occurs in the biologically common regime where the receptor concentration is much smaller than the ligand concentration: $a_0 \ll b_0$. This **pseudo-first-order** (or **ligand excess**) approximation is standard in biochemical kinetics and applies when drug depletion due to target binding is negligible.

Under this assumption, define the dimensionless quantity:

$$x := \frac{4a_0 b_0}{(a_0 + b_0 + K_d)^2}. \tag{22}$$

When $a_0 \ll b_0$, we have $a_0 + b_0 + K_d \approx b_0 + K_d$, so:

$$x \approx \frac{4a_0 b_0}{(b_0 + K_d)^2} \ll 1.$$

For small x, the Taylor expansion $\sqrt{1-x} \approx 1 - x/2 + O(x^2)$ applies. Substituting into (21):

$$\begin{aligned} f_\infty &\approx \frac{b_0 + K_d}{2a_0}\left(1 - \left(1 - \frac{2a_0 b_0}{(b_0+K_d)^2}\right)\right) \\ &\approx \frac{b_0 + K_d}{2a_0} \cdot \frac{2a_0 b_0}{(b_0+K_d)^2} \\ &\approx \frac{b_0}{b_0 + K_d}. \end{aligned} \tag{23}$$

This yields the fundamental result for receptor-ligand binding under pseudo-first-order conditions:

$$\boxed{\mathrm{rEOT}(T) \approx f_\infty \approx \frac{b_0}{K_d + b_0}} \tag{24}$$

Equation (24) is the classical Langmuir isotherm, expressed here as the relative Ehrlich occupancy time. The isotherm exhibits three characteristic regimes: at low drug concentration ($b_0 \ll K_d$), occupancy scales linearly with concentration as $f_\infty \approx b_0/K_d$; at the dissociation constant ($b_0 = K_d$), occupancy reaches its half-maximal value $f_\infty = 1/2$; and at high drug concentration ($b_0 \gg K_d$), occupancy approaches saturation with $f_\infty \to 1$.

Remark 4 (Validity of the Approximation)**.** *The pseudo-first-order approximation requires $a_0 \ll b_0$, ensuring that ligand depletion due to binding is negligible (i.e., $b(t) \approx b_0$ throughout the time course). This condition is typically satisfied in biochemical assays such as SPR and ITC that are designed with excess ligand, in therapeutic settings where drug concentrations (nM–μM) exceed target concentrations, and in cellular assays where receptor density is low relative to extracellular drug. For systems where a_0 and b_0 are comparable, the full expression* (21) *must be used.*

3.1.3 Biological Interpretation

Equation (24) reveals that relative EOT depends on both k_1 and k_2 through the dissociation constant $K_d = k_2/k_1$, not on k_2 alone as in Copeland's DTRT. This represents the correct mathematization of Ehrlich's principle that drugs act when bound—cumulative occupancy at equilibrium is determined by K_d, which emerges naturally from our framework.

While Copeland and coauthors [1] cite Ehrlich, their focus on k_2 alone (DTRT $= 1/k_2$) captures only single-event kinetics, missing the cumulative nature of target engagement that Ehrlich emphasized. The fundamental distinction, visualized in Figure 1, is that Copeland DTRT measures only the duration of individual binding events (panel D), while EOT captures the cumulative occupancy including rebinding (panel C). In closed systems where drug molecules remain available for rebinding after dissociation, EOT provides the complete measure of target engagement.

As illustrated in Figure 1C, every binding event—whether initial or subsequent rebinding—contributes to EOT. The two metrics coincide only when rebinding is absent, as shown in Section 2.4.

3.2 Induced Fit: Conformational Dynamics

Many drug-target interactions involve conformational changes upon binding [14, 15]. The drug may initially bind in one conformation, then induce (or select) a second conformation that alters the stability of the

complex. This **induced fit** mechanism is represented by augmenting the basic binding reaction with an isomerization step:

$$\mathrm{A} + \mathrm{B} \underset{k_2}{\overset{k_1}{\rightleftharpoons}} \mathrm{C} \underset{k_4}{\overset{k_3}{\rightleftharpoons}} \mathrm{D} \tag{25}$$

Here, A is the free receptor, B is the drug, C is the initial encounter complex, and D is the isomerized (conformationally changed) complex. The rate constants k_3 and k_4 govern the forward and reverse isomerization, respectively.

The corresponding mass-action kinetics are:

$$\begin{aligned}
\dot{a} &= -k_1 ab + k_2 c \\
\dot{b} &= -k_1 ab + k_2 c \\
\dot{c} &= k_1 ab - k_2 c - k_3 c + k_4 d \\
\dot{d} &= k_3 c - k_4 d
\end{aligned} \tag{26}$$

The conservation laws are:

$$a + c + d = a_0, \qquad b + c + d = b_0. \tag{27}$$

Since both C and D represent receptor-bound states, the fraction of occupied receptors is:

$$f(t) = \frac{c(t) + d(t)}{a_0}. \tag{28}$$

3.2.1 Equilibrium Analysis

At equilibrium, both reactions are balanced:

$$k_1 a_\infty b_\infty = k_2 c_\infty, \qquad k_3 c_\infty = k_4 d_\infty. \tag{29}$$

From the second condition, the isomerized complex concentration is proportional to the encounter complex:

$$d_\infty = \frac{k_3}{k_4} c_\infty. \tag{30}$$

The total bound receptor concentration is therefore:

$$c_\infty + d_\infty = c_\infty \left(1 + \frac{k_3}{k_4}\right) = c_\infty \cdot \frac{k_3 + k_4}{k_4}. \tag{31}$$

To simplify subsequent expressions, define:

$$\gamma := \frac{k_3 + k_4}{k_4} = 1 + \frac{k_3}{k_4}. \tag{32}$$

Using the conservation laws (27):

$$a_\infty = a_0 - \gamma c_\infty, \qquad b_\infty = b_0 - \gamma c_\infty. \tag{33}$$

Substituting into the first equilibrium condition $k_1 a_\infty b_\infty = k_2 c_\infty$:

$$k_1 (a_0 - \gamma c_\infty)(b_0 - \gamma c_\infty) = k_2 c_\infty. \tag{34}$$

Expanding and rearranging yields a quadratic equation in c_∞:

$$k_1\gamma^2 c_\infty^2 - [k_1\gamma(a_0+b_0)+k_2]c_\infty + k_1 a_0 b_0 = 0. \tag{35}$$

Dividing by $k_1\gamma$ and using $K_d = k_2/k_1$:

$$\gamma c_\infty^2 - (a_0+b_0+\gamma K_d)c_\infty + \frac{a_0 b_0}{\gamma} = 0. \tag{36}$$

The physically meaningful solution (satisfying $0 \le \gamma c_\infty \le \min(a_0, b_0)$) is:

$$c_\infty = \frac{1}{2\gamma}\left(a_0+b_0+\gamma K_d\right)\left(1-\sqrt{1-\frac{4a_0b_0}{(a_0+b_0+\gamma K_d)^2}}\right). \tag{37}$$

3.2.2 Pseudo-First-Order Approximation

For the biologically common case $a_0 \ll b_0$, we apply the same approximation strategy as in Section 3. Define:

$$x := \frac{4a_0b_0}{(a_0+b_0+\gamma K_d)^2} \approx \frac{4a_0b_0}{(b_0+\gamma K_d)^2} \ll 1. \tag{38}$$

Using $\sqrt{1-x} \approx 1 - x/2$ for small x:

$$\begin{aligned} c_\infty &\approx \frac{1}{2\gamma}(b_0+\gamma K_d)\cdot\frac{2a_0b_0}{(b_0+\gamma K_d)^2} \\ &= \frac{a_0b_0}{\gamma(b_0+\gamma K_d)}. \end{aligned} \tag{39}$$

The equilibrium fraction of bound receptors is:

$$\begin{aligned} f_\infty &= \frac{c_\infty + d_\infty}{a_0} = \frac{\gamma c_\infty}{a_0} \\ &= \frac{b_0}{b_0+\gamma K_d} \\ &= \frac{b_0(k_3+k_4)}{b_0(k_3+k_4)+K_d k_4}. \end{aligned} \tag{40}$$

This can be rewritten more elegantly by defining an **effective dissociation constant**:

$$K_d^* := \frac{K_d}{\gamma} = \frac{K_d}{1+k_3/k_4} = \frac{k_2k_4}{k_1(k_3+k_4)}. \tag{41}$$

With this definition, the equilibrium occupancy takes the familiar Langmuir form:

$$\boxed{f_\infty = \frac{b_0}{K_d^* + b_0}} \tag{42}$$

Since $\gamma \ge 1$ (with equality only when $k_3 = 0$), we have $K_d^* \le K_d$. The induced fit mechanism effectively *increases* the apparent binding affinity.

3.2.3 Clinical Examples of Induced Fit

The induced fit mechanism is not merely theoretical—it has been exploited successfully in drug design.

Example 2 (Type II Kinase Inhibitors)**.** *Imatinib (Gleevec), used to treat chronic myeloid leukemia, binds to the BCR-ABL kinase in an inactive "DFG-out" conformation. Upon binding, the drug stabilizes a conformational state (complex D) that differs from the initial encounter complex (complex C). This conformational selection mechanism contributes to imatinib's prolonged residence time (∼30 minutes) despite moderate equilibrium affinity [8]. In our framework, a large k_3/k_4 ratio (favoring the DFG-out state) reduces K_d^* below the intrinsic K_d, enhancing target occupancy.*

Example 3 (GPCR Ligands)**.** *Many G protein-coupled receptor (GPCR) drugs induce conformational changes that stabilize active or inactive receptor states. Tiotropium, a long-acting muscarinic antagonist for COPD, exhibits slow dissociation ($k_2 \sim 0.0002\ s^{-1}$, residence time ∼1.4 hours) partly due to conformational stabilization of an inactive receptor state. This allows once-daily dosing despite systemic elimination within hours.*

These examples demonstrate that optimizing the conformational landscape (large k_3/k_4) can achieve prolonged target occupancy even when initial binding (k_1, k_2) is not exceptionally favorable.

3.2.4 Biological Interpretation

The conformational change acts as a kinetic "trap." Fast forward isomerization (large k_3) or slow reverse isomerization (small k_4) increases the ratio k_3/k_4, thereby decreasing K_d^* and increasing rEOT. This explains why induced fit inhibitors can achieve prolonged target occupancy even with moderate initial binding affinity.

To illustrate the magnitude of this effect, consider two limiting scenarios. In the absence of induced fit ($k_3 = 0$), the effective dissociation constant reduces to $K_d^* = K_d$, recovering simple binding behavior. With a strong induced fit ($k_3/k_4 = 9$), however, the effective dissociation constant becomes $K_d^* = K_d/10$, representing a 10-fold increase in apparent affinity purely from conformational trapping.

The framework quantifies how conformational dynamics contribute to residence time beyond simple binding kinetics.

Example 4 (Quantitative Impact)**.** *Suppose $K_d = 1\ \mu M$ and $b_0 = 1\ \mu M$. Without induced fit, $K_d^* = K_d = 1\ \mu M$, yielding $f_\infty = 1/(1+1) = 0.50$. With a strong induced fit ($k_3/k_4 = 9$), the effective dissociation constant drops to $K_d^* = 0.1\ \mu M$, yielding $f_\infty = 1/(0.1+1) \approx 0.91$. Thus, the induced fit mechanism increases target occupancy from 50% to 91%—an 82% relative increase—purely from conformational trapping, without changing the intrinsic binding rate constants k_1 and k_2.*

Our finding that induced fit mechanisms can dramatically extend occupancy time is consistent with Copeland's recent acknowledgment of conformational dynamics in residence time [16]. However, our framework quantifies this effect through the modified dissociation constant $K_d^* = K_d/(1 + k_3/k_4)$, providing a direct mathematical relationship between conformational kinetics and occupancy time.

Remark 5 (Notation for k_3)**.** *In this section, k_3 denotes the forward isomerization rate constant. In Section 4, k_3 will denote the drug elimination rate constant. These are distinct parameters appearing in different reaction mechanisms. The context (induced fit vs. drug removal) determines which meaning applies.*

4 Ehrlich Occupancy Time with Drug Removal

4.1 Biological Motivation

In vivo, drugs undergo continuous removal through metabolism, renal excretion, and other elimination processes. These pharmacokinetic factors fundamentally alter drug-target interactions by depleting the free drug pool available for binding. Unlike closed systems where EOT grows linearly with time, drug removal causes EOT to saturate at a finite limit EOT_∞ as $T \to \infty$. Understanding this limit is crucial for predicting therapeutic duration and optimizing dosing regimens.

To illustrate the magnitude of these effects, consider a hypothetical drug with strong target binding ($K_d = 1$ nM, $k_2 = 0.001$ s^{-1}) administered intravenously at a dose achieving the initial plasma concentration $b_0 = 100$ nM. With slow elimination ($k_3 = 0.0001$ s^{-1}, corresponding to $t_{1/2} \sim 2$ hours), the upper bound from equation (56) gives $\mathrm{EOT}^u_\infty = 100/(1 \times 0.0001) = 10^6$ nM·s, and target occupancy remains high over a 24-hour period. In stark contrast, with rapid elimination ($k_3 = 0.1$ s^{-1}, $t_{1/2} \sim 7$ seconds), the upper bound drops to $\mathrm{EOT}^u_\infty = 1000$ nM·s—three orders of magnitude lower despite identical binding kinetics. Despite identical binding kinetics, rapid clearance limits effective target engagement to minutes rather than hours.

This 1000-fold difference cannot be predicted from binding affinity or Copeland DTRT alone. It explains why some high-affinity compounds discovered in biochemical assays fail in vivo: excellent target binding is negated by poor pharmacokinetics. Our framework quantifies this interplay explicitly.

4.2 Model Formulation

Consider receptor-ligand binding coupled with first-order drug removal:

$$\begin{aligned} \mathrm{A} + \mathrm{B} &\underset{k_2}{\overset{k_1}{\rightleftharpoons}} \mathrm{C} \\ \mathrm{B} &\xrightarrow{k_3} \varnothing \end{aligned} \tag{43}$$

Here k_3 represents the first-order elimination rate constant, encompassing all removal processes (metabolism, excretion, distribution out of the compartment). The mass-action equations are:

$$\begin{aligned} \dot{a} &= -k_1 ab + k_2 c \\ \dot{b} &= -k_1 ab + k_2 c - k_3 b \\ \dot{c} &= k_1 ab - k_2 c \end{aligned} \tag{44}$$

with initial conditions $a(0) = a_0$, $b(0) = b_0$, $c(0) = 0$. The conservation law $a + c = a_0$ still holds (receptor is conserved), but total ligand is no longer conserved due to elimination.

Unlike closed systems, $b(t) \to 0$ as $t \to \infty$ due to removal, driving the system toward complete dissociation ($c(t) \to 0$). Consequently, $\mathrm{EOT}(T)$ approaches a finite limit EOT_∞ rather than growing indefinitely.

4.2.1 Comparison with the DTRT Approach

To illustrate the limitations of Copeland's DTRT approach in this context, consider what happens if we apply the DTRT methodology to our system. Following Copeland et al. [1], one would wait for the system to reach a quasi-steady state (a^*, b^*, c^*) with positive entries, then "switch off" ligand association (mimicking infinite

dilution). The remaining dynamics are:

$$\begin{aligned} \dot{a} &= k_2 c \\ \dot{b} &= -k_3 b + k_2 c \\ \dot{c} &= -k_2 c \end{aligned} \tag{45}$$

This linear system has eigenvalues 0, $-k_3$, and $-k_2$. While the complete system dynamics are governed by the smaller of k_2 and k_3, the DTRT approach focuses solely on the third equation, concluding that k_2 alone determines residence time (DTRT $= 1/k_2$).

This analysis reveals three critical limitations of the DTRT approach. First, DTRT neglects the elimination rate k_3 entirely, yet when $k_3 > k_2$, drug elimination dominates the long-term behavior and determines the duration of target engagement. Second, by assuming infinite dilution, DTRT cannot capture rebinding events—the reassociation of dissociated drug molecules with nearby targets—that can substantially extend occupancy in vivo. Third, the single-parameter metric ($1/k_2$) fundamentally cannot capture the multi-parameter dependencies revealed by our EOT framework, where both binding kinetics and pharmacokinetics jointly determine cumulative occupancy.

Our EOT analysis shows that both k_2 and k_3 contribute to determining occupancy time, with their relative importance determined by the ratio k_3/k_2.

4.3 Pseudo-First-Order Approximation

The system (44) does not admit a closed-form solution in general. However, under the assumption of excess ligand ($a_0 \ll b_0$), we can derive a tractable approximation. This assumption is standard in many experimental and therapeutic settings: therapeutic plasma concentrations typically range from nanomolar to micromolar, while many drug targets exist at substantially lower concentrations (e.g., intracellular kinases are often present at only 1–100 nM), and biochemical binding assays such as SPR and ITC are typically designed with excess ligand to ensure measurable signals. The approximation is valid whenever drug depletion due to target binding is negligible, i.e., when the amount of drug bound to targets remains small compared to the total amount of drug present.

4.3.1 Derivation of the Reduced System

For pseudo-first-order conditions, we scale the receptor concentration as $a_0 = \varepsilon \hat{a}_0$ where $\varepsilon \ll 1$. The conservation law $a + c = a_0$ implies that both a and c remain of order ε for all time. Scaling $a = \varepsilon \hat{a}$ and $c = \varepsilon \hat{c}$, the system (44) becomes:

$$\begin{aligned} \dot{\hat{a}} &= -k_1 \hat{a} b + k_2 \hat{c} \\ \dot{b} &= -k_3 b + \varepsilon(-k_1 \hat{a} b + k_2 \hat{c}) \\ \dot{\hat{c}} &= k_1 \hat{a} b - k_2 \hat{c} \end{aligned}$$

To leading order in ε (i.e., ignoring the $O(\varepsilon)$ terms in the second equation), the ligand dynamics decouple:

$$\dot{b} = -k_3 b, \qquad b(0) = b_0, \tag{46}$$

with solution:

$$b(t) = b_0 \exp(-k_3 t). \tag{47}$$

Substituting into the equation for the complex and using $\hat{c} = c/\varepsilon$, $\hat{a}_0 = a_0/\varepsilon$, we obtain (after multiplying through by ε):

$$\dot{c} = k_1(a_0 - c)b(t) - k_2 c = k_1(a_0 - c)b_0 \exp(-k_3 t) - k_2 c. \tag{48}$$

Rearranging:

$$\boxed{\dot{c} = -[k_1 b_0 \exp(-k_3 t) + k_2]c + k_1 a_0 b_0 \exp(-k_3 t), \qquad c(0) = 0} \tag{49}$$

This is a linear, non-autonomous first-order ODE. The Ehrlich occupancy time is:

$$\mathrm{EOT}(T) = \frac{1}{a_0} \int_0^T c(t)\,\mathrm{d}t, \tag{50}$$

and we seek $\mathrm{EOT}_\infty = \lim_{T\to\infty} \mathrm{EOT}(T)$.

4.3.2 Solution Structure

The solution to (49) can be expressed using variation of constants. The homogeneous equation $\dot{v} = -[k_1 b_0 \exp(-k_3 t) + k_2]v$ has solution:

$$v(t) = \exp\left(\frac{k_1 b_0}{k_3}(\exp(-k_3 t) - 1) - k_2 t\right). \tag{51}$$

While this leads to an exact integral representation of $c(t)$, the resulting integrals generally cannot be evaluated in closed form. Instead, we derive rigorous upper and lower bounds using comparison principles for differential equations [17].

4.4 Analytical Bounds for EOT_∞

4.4.1 Upper Bound via Comparison Principle

From equation (49), since $c \geq 0$ and $\exp(-k_3 t) \leq 1$ for $t \geq 0$, we have the differential inequality:

$$\dot{c} \leq -k_2 c + k_1 a_0 b_0 \exp(-k_3 t). \tag{52}$$

Consider the comparison equation:

$$\dot{w} = -k_2 w + k_1 a_0 b_0 \exp(-k_3 t), \qquad w(0) = 0. \tag{53}$$

This is a linear first-order ODE, which we solve using the integrating factor $\mu(t) = \exp(k_2 t)$:

$$\frac{\mathrm{d}}{\mathrm{d}t}[\exp(k_2 t)w] = k_1 a_0 b_0 \exp((k_2 - k_3)t).$$

Integrating from 0 to t (assuming $k_2 \neq k_3$; the borderline case yields the same final bounds):

$$\exp(k_2 t)w(t) = k_1 a_0 b_0 \int_0^t \exp((k_2 - k_3)s)\,\mathrm{d}s = \frac{k_1 a_0 b_0}{k_2 - k_3}[\exp((k_2 - k_3)t) - 1].$$

Therefore:

$$w(t) = \frac{k_1 a_0 b_0}{k_2 - k_3}[\exp(-k_3 t) - \exp(-k_2 t)]. \tag{54}$$

By the comparison principle for differential inequalities [17], since $c(0) = w(0) = 0$ and $\dot{c} \leq -k_2 c + k_1 a_0 b_0 \exp(-k_3 t) = \dot{w} + k_2(w - c)$, we have $c(t) \leq w(t)$ for all $t \geq 0$. To obtain the bound on EOT_∞, we integrate:

$$\begin{aligned}\mathrm{EOT}_\infty &= \frac{1}{a_0}\int_0^\infty c(t)\,\mathrm{d}t \leq \frac{1}{a_0}\int_0^\infty w(t)\,\mathrm{d}t \\ &= \frac{k_1 b_0}{k_2 - k_3}\int_0^\infty [\exp(-k_3 t) - \exp(-k_2 t)]\,\mathrm{d}t. \end{aligned} \tag{55}$$

Using the standard result $\int_0^\infty [\exp(-\alpha t) - \exp(-\beta t)]\,\mathrm{d}t = 1/\alpha - 1/\beta = (\beta - \alpha)/(\alpha\beta)$ for $\alpha, \beta > 0$:

$$\int_0^\infty [\exp(-k_3 t) - \exp(-k_2 t)]\,\mathrm{d}t = \frac{k_2 - k_3}{k_2 k_3}.$$

Substituting:

$$\mathrm{EOT}_\infty \leq \frac{k_1 b_0}{k_2 - k_3} \cdot \frac{k_2 - k_3}{k_2 k_3} = \frac{k_1 b_0}{k_2 k_3}.$$

Expressing in terms of $K_d = k_2/k_1$:

$$\boxed{\mathrm{EOT}_\infty \leq \frac{k_1 b_0}{k_2 k_3} = \frac{b_0}{K_d \cdot k_3} =: \mathrm{EOT}_\infty^u} \tag{56}$$

4.4.2 Lower Bound via Comparison Principle

From equation (49), since $\exp(-k_3 t) \leq 1$ and $c \geq 0$:

$$\dot{c} \geq -(k_1 b_0 + k_2)c + k_1 a_0 b_0 \exp(-k_3 t). \tag{57}$$

Consider the comparison equation:

$$\dot{v} = -(k_1 b_0 + k_2)v + k_1 a_0 b_0 \exp(-k_3 t), \qquad v(0) = 0. \tag{58}$$

Using the integrating factor $\mu(t) = \exp((k_1 b_0 + k_2)t)$:

$$\frac{\mathrm{d}}{\mathrm{d}t}[\exp((k_1 b_0 + k_2)t)v] = k_1 a_0 b_0 \exp((k_1 b_0 + k_2 - k_3)t).$$

Integrating from 0 to t:

$$v(t) = \frac{k_1 a_0 b_0}{k_1 b_0 + k_2 - k_3}[\exp(-k_3 t) - \exp(-(k_1 b_0 + k_2)t)].$$

By the comparison principle, $c(t) \geq v(t)$ for all $t \geq 0$. Integrating over $[0, \infty)$:

$$\begin{aligned}
\mathrm{EOT}_\infty &\geq \frac{1}{a_0} \int_0^\infty v(t)\,\mathrm{d}t \\
&= \frac{k_1 b_0}{k_1 b_0 + k_2 - k_3} \int_0^\infty [\exp(-k_3 t) - \exp(-(k_1 b_0 + k_2)t)]\,\mathrm{d}t \\
&= \frac{k_1 b_0}{k_1 b_0 + k_2 - k_3} \cdot \frac{k_1 b_0 + k_2 - k_3}{k_3(k_1 b_0 + k_2)} \\
&= \frac{k_1 b_0}{k_3(k_1 b_0 + k_2)}. \qquad (59)
\end{aligned}$$

Expressing in terms of K_d:

$$\boxed{\mathrm{EOT}_\infty \geq \frac{k_1 b_0}{(k_1 b_0 + k_2)k_3} = \frac{b_0}{(b_0 + K_d)k_3} =: \mathrm{EOT}_\infty^l} \qquad (60)$$

4.4.3 Summary of Bounds

Combining equations (56) and (60):

$$\boxed{\frac{b_0}{(b_0 + K_d)k_3} \leq \mathrm{EOT}_\infty \leq \frac{b_0}{K_d \cdot k_3}} \qquad (61)$$

The relationship between the bounds can be expressed as:

$$\frac{1}{\mathrm{EOT}_\infty^l} = 1 + \frac{k_3 K_d}{b_0} = 1 + \frac{1}{\mathrm{EOT}_\infty^u}. \qquad (62)$$

The ratio of upper to lower bounds is:

$$\frac{\mathrm{EOT}_\infty^u}{\mathrm{EOT}_\infty^l} = \frac{b_0 + K_d}{K_d} = 1 + \frac{b_0}{K_d}. \qquad (63)$$

4.4.4 Sharpness of the Bounds

The bounds (61) are tightest when $b_0 \ll K_d$ (low drug concentration relative to affinity), where $\mathrm{EOT}_\infty^u / \mathrm{EOT}_\infty^l \approx 1$. The bounds diverge when $b_0 \gg K_d$ (high concentration), but in this regime both bounds predict large EOT_∞, so the qualitative conclusion (prolonged occupancy) remains valid.

More precisely, we can compare two sets of bounds. The *standard bounds* (equations (56)–(60)), derived above using comparison with constant-coefficient equations, are complemented by *exponential bounds* derived using variation of constants (Appendix A). The exponential bounds take the form:

$$\exp\left(-\frac{k_1 b_0}{k_3}\right) \frac{b_0}{K_d k_3} \leq \mathrm{EOT}_\infty \leq \exp\left(\frac{k_1 b_0}{k_3}\right) \frac{b_0}{K_d k_3}. \qquad (64)$$

The standard upper bound is always tighter than the exponential upper bound. For the lower bounds, the standard bound is tighter when:

$$\frac{k_2}{k_1 b_0 + k_2} \geq \exp\left(-\frac{k_1 b_0}{k_3}\right),$$

which is satisfied whenever $k_2 > k_3$. Since the biologically common regime has dissociation faster than elimination ($k_2 > k_3$), the standard bounds (61) are typically the most useful.

4.5 Biological Interpretation

4.5.1 Effect of Removal Rate k_3

Both bounds are inversely proportional to k_3. Faster drug elimination (larger k_3) proportionally reduces EOT_∞. This reveals a fundamental trade-off: even drugs with very slow dissociation (small k_2, large Copeland DTRT) achieve only limited target occupancy if eliminated rapidly. For example, if $k_3 \gg k_2$, removal dominates and EOT_∞ is primarily limited by pharmacokinetics rather than binding kinetics. From equation (56), doubling k_3 halves the maximum achievable EOT_∞ regardless of binding affinity.

Rebinding in the presence of elimination. The interplay between rebinding and drug removal deserves special attention. In a closed system (Section 3), a dissociated drug molecule remains available indefinitely for rebinding, leading to multiple occupancy cycles as depicted in Figure 1C. With drug removal, however, each dissociation event is potentially final: the probability that a dissociated drug molecule rebinds before being eliminated is approximately $k_1 b(t)/(k_1 b(t) + k_3)$.

As drug concentration $b(t) = b_0 \exp(-k_3 t)$ declines exponentially, this probability decreases over time. Early in the time course, when $b(t) \approx b_0$, rebinding remains likely and the system exhibits dynamics similar to the closed case. At later times, when $b(t) \ll K_d$, rebinding becomes rare, and the system approaches the Copeland limit where each receptor experiences at most one binding event.

This temporal evolution from a rebinding-dominated regime to a single-binding regime explains why our bounds depend on both K_d and k_3: they capture the full spectrum of behaviors across the entire time course.

4.5.2 Effect of Dissociation Constant K_d

The upper bound $\mathrm{EOT}_\infty^u = b_0/(K_d k_3)$ shows that tighter binding (smaller K_d) increases occupancy time, as expected. However, the lower bound $\mathrm{EOT}_\infty^l = b_0/[(b_0 + K_d)k_3]$ reveals more nuanced behavior depending on drug concentration relative to affinity. Under saturating conditions ($b_0 \gg K_d$), the lower bound simplifies to $\mathrm{EOT}_\infty^l \approx 1/k_3$, becoming independent of binding affinity—once targets are saturated, occupancy duration is determined entirely by how long drug remains available. Conversely, under subsaturating conditions ($b_0 \ll K_d$), the lower bound becomes $\mathrm{EOT}_\infty^l \approx (k_1 b_0)/(k_2 k_3)$, showing that both association and dissociation rates contribute to determining occupancy time.

4.5.3 Parameter Regimes

We identify three key regimes based on the ratio k_3/k_2:

1. $k_3 \ll k_2$ **(slow removal):** Drug clearance is slower than unbinding. EOT_∞ is primarily determined by binding kinetics, and the system behaves similarly to a closed system over therapeutically relevant timescales. The upper bound dominates: $\mathrm{EOT}_\infty \approx b_0/(K_d k_3)$.

2. $k_3 \approx k_2$ **(comparable rates):** Both binding kinetics and pharmacokinetics contribute significantly. The bounds (61) provide tight estimates. Optimization requires balancing affinity and elimination rate.

3. $k_3 \gg k_2$ **(fast removal):** Drug is eliminated before significant binding equilibration. The lower bound dominates: $\mathrm{EOT}_\infty \approx b_0/[(b_0 + K_d)k_3]$. In this regime, improving binding affinity has limited benefit unless k_3 is also reduced (e.g., via formulation changes, prodrugs, or reducing first-pass metabolism).

Decision framework for drug optimization. The bounds (61) provide actionable guidance for medicinal chemistry optimization, as summarized in Table 2. Appendix B provides detailed experimental protocols for measuring the required parameters and a case study illustrating this optimization workflow.

Table 2: Decision framework for drug optimization based on EOT analysis.

Observation	**Diagnosis**	**Optimization Strategy**
Low cellular potency despite good biochemical K_d	Likely $k_3 \gg k_2$: fast removal limits occupancy	Reduce k_3 by minimizing metabolic soft spots or blocking efflux transporters; increase k_2^{-1} by optimizing for slower dissociation
Strong biochemical but weak in vivo efficacy	k_3 limits EOT_∞ despite good K_d	Consider formulation strategies (sustained release), prodrug approaches, or combination with metabolic inhibitors to reduce effective k_3
Good potency but short duration of action	Slow off-rate (k_2^{-1}) not compensating for large k_3	Prioritize compounds with ultra-slow k_2 or explore covalent inhibitors (irreversible binding)
Adequate efficacy but requiring frequent dosing	EOT_∞ sufficient but duration limited by k_3	Optimize PK profile rather than binding kinetics; consider depot formulations

4.6 Comparison with Copeland DTRT

Copeland's framework defines $\mathrm{DTRT} = 1/k_2$, independent of k_3. This predicts that two drugs with identical k_2 but different k_3 values would have identical residence times—clearly incorrect in vivo. Our EOT framework correctly predicts that faster elimination (larger k_3) reduces occupancy time proportionally, regardless of k_2.

The conceptual limitation of Copeland DTRT becomes particularly apparent in the drug removal scenario. As shown in Figure 1D, Copeland's approach counts only the duration of the first binding event for each receptor. However, in the presence of drug removal, whether a receptor experiences subsequent binding events (Figure 1C) depends critically on k_3: fast elimination reduces the likelihood of rebinding by depleting available drug molecules. Since Copeland DTRT ignores rebinding entirely by definition, it cannot capture this pharmacokinetic effect.

Example 5 (Comparison of Two Drugs)**.** *Consider two drugs with identical association and dissociation kinetics ($k_1 = 10^6\ M^{-1}s^{-1}$, $k_2 = 0.1\ s^{-1}$) but different elimination rates: Drug A has slow elimination ($k_3 = 0.01\ s^{-1}$) while Drug B has rapid elimination ($k_3 = 1.0\ s^{-1}$). Both drugs have identical $K_d = 0.1$ μM and Copeland DTRT of 10 s. However, applying equation* (56)*, Drug A achieves* $\mathrm{EOT}^u_\infty = 10^9 b_0$ *while*

Drug B achieves only $\mathrm{EOT}^u_\infty = 10^7 b_0$*—a 100-fold difference in cumulative target occupancy that is entirely invisible to the Copeland framework but crucial for predicting in vivo efficacy.*

TABLE 3 provides additional comparative examples that illustrate how Copeland DTRT can be misleading when elimination rates differ.

Table 3: Example calculations comparing Copeland DTRT and EOT_∞ for hypothetical drugs.

Drug	k_1 ($\mathrm{M}^{-1}\mathrm{s}^{-1}$)	k_2 (s^{-1})	k_3 (s^{-1})	K_d (μM)	**Copeland DTRT (s)**	**EOT^u_∞ at $b_0 = 10\,\mu$M (s)**
A	10^6	0.1	0.01	0.1	10	10,000
B	10^6	0.1	1.0	0.1	10	100
C	10^5	0.01	0.01	0.1	100	10,000
D	10^5	0.01	1.0	0.1	100	100

Interpretation: Drugs A and B have identical Copeland DTRT but 100-fold different EOT_∞ due to elimination rate differences. Drugs A and C have identical EOT_∞ despite 10-fold different Copeland DTRT. This demonstrates that Copeland DTRT alone cannot predict in vivo occupancy time when drug elimination is significant.

4.7 Numerical Validation

FIGURES 2 and 3 present extensive numerical simulations validating our theoretical bounds across a comprehensive parameter space. We solve the full system (44) numerically for over 1,600 parameter combinations and compare with bounds (61).

4.7.1 Computational Approach

The simulations span k_3/k_2 ratios from 0.01 to 100 (four orders of magnitude) and b_0/K_d ratios from 0.1 to 50 (sub-saturating to saturating regimes). Computations were performed on a 40×40 parameter grid with bicubic interpolation to 200×200 for visualization. Throughout, validity of the pseudo-first-order approximation was ensured by maintaining $a_0/b_0 \leq 0.01$.

4.7.2 Key Observations

The numerical results (FIGURE 2) confirm that our analytical bounds bracket the true EOT_∞ across all parameter regimes tested. The upper bound is tightest when $b_0 \ll K_d$ (panels B and D, blue regions), while the lower bound is tightest when $b_0 \gg K_d$ (panels C and D, red regions). Both bounds converge in extreme regimes where either $k_3 \ll k_2$ or $k_3 \gg k_2$ (panel E), and overall the bounds remain valid across six orders of magnitude in parameter space.

FIGURE 3 further demonstrates the time evolution and parameter dependencies, showing that $\mathrm{EOT}(t)$ approaches EOT_∞ within the analytical bounds when the pseudo-first-order approximation is satisfied (panels D–F).

5 Discussion

We have presented a mathematically rigorous framework for *Ehrlich occupancy time* (EOT) that unifies classical residence-time concepts with dynamic ligand availability and conformational change. The central

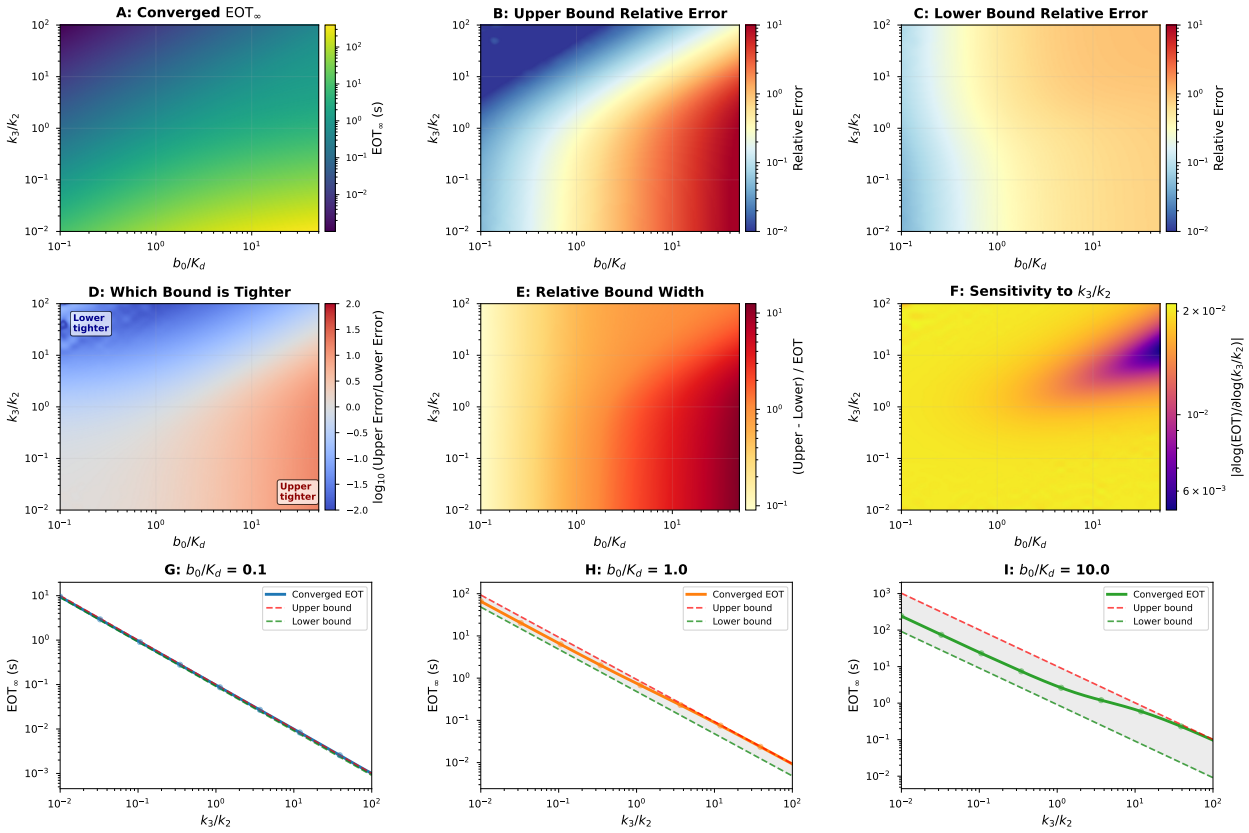

Figure 2: **High-resolution analysis of EOT bounds across parameter space. (A)** Converged EOT_∞ values showing the full landscape of occupancy times across four orders of magnitude in k_3/k_2 and nearly two orders in b_0/K_d. **(B)** Upper bound relative error, demonstrating the bound is tightest (error < 0.1) when $b_0 \ll K_d$ (low drug concentration regime). **(C)** Lower bound relative error, demonstrating the bound is tightest when $b_0 \gg K_d$ (saturation regime). **(D)** Bound tightness comparison map, where blue regions indicate the lower bound is closer to the exact solution and red regions indicate the upper bound is closer. **(E)** Relative bound width $(\mathrm{EOT}_\infty^u - \mathrm{EOT}_\infty^l)/\mathrm{EOT}_\infty$, showing the bounds are most precise at extreme k_3/k_2 values. **(F)** Sensitivity analysis showing $|\partial \log(\mathrm{EOT})/\partial \log(k_3/k_2)|$, identifying regions of high parameter sensitivity. **(G-I)** Line plots of EOT_∞ vs k_3/k_2 for $b_0/K_d = \{0.1, 1.0, 10.0\}$ respectively, with computed data points (dots, every 5th point shown), smooth interpolated curves (solid lines), upper bounds (red dashed), lower bounds (green dashed), and shaded gray regions indicating the valid bound range. The bounds provide reliable estimates across six orders of magnitude in both parameters. All simulations maintain pseudo-first-order validity ($a_0/b_0 \leq 0.01$) to ensure bound accuracy. The heatmaps are computed on a 40×40 grid and displayed with 200×200 bicubic interpolation for smooth visualization.

definition, $\mathrm{EOT}(T) = \int_0^T f(t)\,\mathrm{d}t$ where $f(t)$ is the fraction of occupied receptors at time t, captures cumulative occupancy including rebinding events and drug elimination effects—features absent from Copeland's drug-target residence time ($\mathrm{DTRT} = 1/k_2$), which considers only the lifetime of a single binding event.

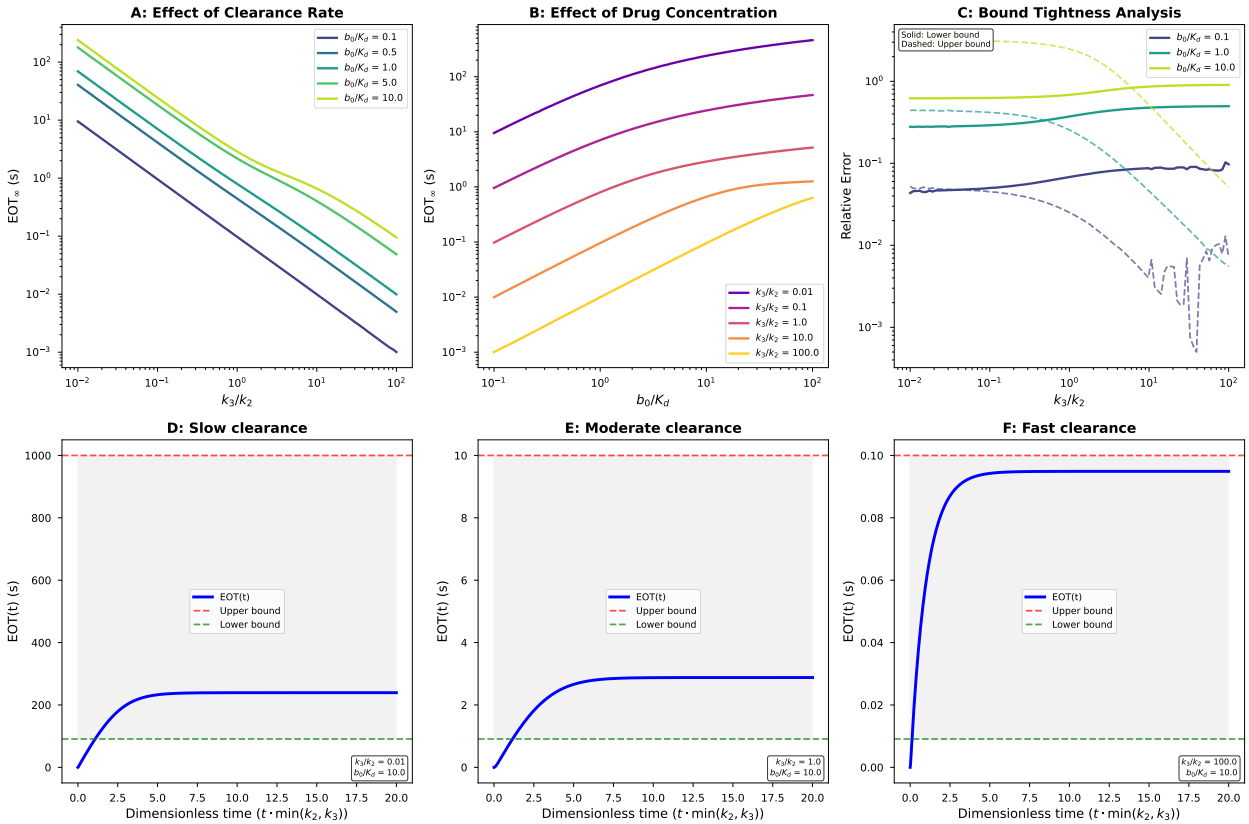

Figure 3: **Systematic analysis of EOT behavior and bound quality.** **(A)** Effect of clearance rate: EOT_∞ vs k_3/k_2 for different drug concentrations ($b_0/K_d = 0.1$ to 10), showing the transition from dissociation-limited (left) to clearance-limited (right) regimes. **(B)** Effect of drug concentration: EOT_∞ vs b_0/K_d for different k_3/k_2 ratios. **(C)** Bound tightness analysis showing relative error of upper (dashed) and lower (solid) bounds across parameter space. **(D–F)** Time evolution of $\mathrm{EOT}(t)$ approaching EOT_∞ for three representative clearance rates at fixed $b_0/K_d = 10$: (D) slow clearance ($k_3/k_2 = 0.01$), (E) moderate clearance ($k_3/k_2 = 1$), and (F) fast clearance ($k_3/k_2 = 100$). Blue curves show numerical $\mathrm{EOT}(t)$, horizontal dashed lines indicate analytical bounds (red: upper, green: lower), and gray shading shows the bound region. Panels D–F maintain pseudo-first-order validity ($a_0/b_0 = 0.01$), ensuring the analytical bounds are accurate.

In closed systems approaching equilibrium, we proved that relative EOT converges to the equilibrium occupancy fraction $f_\infty = b_0/(K_d + b_0)$, depending on the dissociation constant $K_\mathrm{d} = k_2/k_1$ rather than on k_2 alone. For induced-fit mechanisms, conformational trapping reduces the effective dissociation constant to $K_d^* = K_d/(1+k_3/k_4)$, providing a quantitative link between conformational kinetics and prolonged occupancy.

In open systems with first-order drug elimination at rate k_3, we derived rigorous bounds:

$$\frac{b_0}{(b_0 + K_d)k_3} \leq \mathrm{EOT}_\infty \leq \frac{b_0}{K_d \cdot k_3},$$

demonstrating that long-time occupancy is governed jointly by binding affinity and elimination rate. The

numerical validation (FIGURES 2 and 3) confirms that these bounds bracket the true EOT_∞ across six orders of magnitude in parameter space, with the bounds tightest when $b_0 \ll K_d$ (upper bound) or $b_0 \gg K_d$ (lower bound).

5.1 Relation to Existing Residence-Time Metrics

Our framework contains Copeland's DTRT as a limiting case: when ligand is abundant and effectively constant, target turnover is negligible, and no induced-fit penalty applies, EOT reduces to DTRT. Outside this regime—particularly when exposure decays on the same timescale as dissociation, or when conformational gating is operative—DTRT misestimates the pharmacologically relevant occupancy time. In contrast, EOT is *exposure-aware* and *mechanism-aware*, incorporating association, dissociation, rebinding, conformational isomerization, and drug elimination within a single analytic scheme. TABLE 4 summarizes the key differences.

Table 4: Comparison of residence time definitions.

Feature	**Copeland DTRT**	**Ehrlich EOT (This Work)**
Mathematical definition	$1/k_{\mathrm{off}}$	$\int_0^T f(t)\,\mathrm{d}t$
Depends on k_{on}	No	Yes
Includes rebinding	No[a]	Yes
Accounts for drug removal	No	Yes
Handles conformational change	Limited[b]	Yes (eq. (42))
Closed-form solution	Always	Closed systems only
Bounds for open systems	N/A	Equations (61)
Valid when $k_3 > k_2$	No	Yes
Predicts in vivo efficacy	Limited	Improved

[a] Recent work acknowledges rebinding importance [16] but does not quantify it.
[b] An expression for k_{off} is indicated in [1]; it does not incorporate rebinding.

Recent developments in residence-time theory have moved toward acknowledging these complexities. Copeland's 2021 review [16] recognizes that intracellular residence time depends on the association rate constant and that cellular residence times are often prolonged by rebinding cycles. Our EOT framework quantifies these effects explicitly through the concentration-dependent terms in our bounds. Similarly, Folmer's critique [12] that residence time provides a limited view of binding kinetics is addressed by our multi-parameter approach incorporating k_1, k_2, k_3, and b_0.

5.2 Implications for Drug Design

A central parameter emerging from our analysis is the dimensionless ratio k_3/k_2. When this ratio is small (drug persists longer than the complex lifetime), extending residence time by reducing k_2 materially increases cumulative occupancy. When k_3/k_2 is moderate to large (exposure decays quickly relative to dissociation), modulating exposure—via formulation, dosing schedule, or distribution to protected compartments—dominates efficacy. The EOT_∞-versus-(k_3/k_2) curves (FIGURE 2, panels G–I) quantify how much improvement is available from each optimization strategy.

These findings have several practical implications. First, binding affinity alone is insufficient for predicting efficacy: two drugs with identical K_d can have vastly different EOT values if their individual rate constants (k_1, k_2) or elimination rates (k_3) differ. Second, pharmacokinetics and pharmacodynamics are inseparable when predicting target occupancy—the bounds show that k_3 (a PK parameter) and K_d (a PD parameter) contribute multiplicatively, so optimizing one while neglecting the other may yield no net benefit. Third, for targets exhibiting induced fit, compounds triggering favorable conformational changes can achieve prolonged occupancy through kinetic trapping even with moderate initial binding affinity.

For experimentalists, the EOT framework provides concrete, testable targets: measuring k_1 and k_2 under conditions representing the biological compartment, characterizing the effective elimination rate k_3, and identifying induced-fit signatures from multiphasic dissociation kinetics. Appendix B provides detailed protocols for these measurements along with a case study workflow for drug optimization.

5.3 Common Misconceptions

Based on discussions with experimental collaborators, we address three frequent misunderstandings.

First, *high affinity does not automatically imply long occupancy time.* While low K_d increases equilibrium occupancy, cumulative EOT depends additionally on elimination rate. A high-affinity drug can have short EOT if eliminated rapidly, because the system never reaches equilibrium before clearance. This explains why some high-affinity compounds fail in vivo despite excellent biochemical profiles.

Second, *Copeland residence time does not predict in vivo duration* in general. DTRT $= 1/k_2$ measures the lifetime of a single binding event, whereas in vivo duration depends on EOT, which includes rebinding and elimination. As shown in Table 3, drugs with identical DTRT can have 100-fold different EOT due to differences in k_3.

Third, *slow off-rate is not always beneficial.* Slow k_2 helps only if drug remains available for binding; when $k_3 \gg k_2$, elimination dominates and further reducing k_2 provides diminishing returns. Moreover, extremely slow dissociation can cause on-target toxicity, reduce dose titratability, slow onset of action, or provide no benefit when target turnover is rapid. The optimal strategy is to match residence time to the desired therapeutic duration, considering target turnover and dosing frequency.

5.4 Limitations and Future Directions

We have idealized several processes as first-order (clearance, turnover) and treated induced fit via reduced-order kinetics. In compartments with transport bottlenecks or anomalous diffusion, or in systems with cooperative assembly, effective rates may be time-dependent. Extending the theory to such non-Markovian dynamics—for example, using memory kernels or distributed delays—is feasible and would refine long-time predictions. Target heterogeneity and spatial microdomains can be represented by mixture models, though careful experimental design remains essential.

Looking forward, EOT offers an exposure-aware, mechanism-aware calculus for target engagement. The monotone dependence of EOT_∞ on k_3/k_2 yields an operative design principle: match medicinal-chemistry effort (on k_2) and formulation/PK effort (on k_3) to the regime the system inhabits, rather than optimizing one axis in isolation. Coupling this framework to standard PK/PD models should produce tractable rules for dosage, scheduling, and scaffold selection, with clear, testable predictions across parameter domains.

Author Contributions Statement

J.E., S.S. and S.W. made substantial contributions to the conception and design of the work, analysis and interpretation of the results. S.S., S.W. and J.E. wrote the manuscript and S.S. and J.E. prepared the figures. All authors reviewed and approved the manuscript.

References

[1] R. A. Copeland, D. L. Pompliano, and T. D. Meek. Drug-target residence time and its implications for lead optimization. *Nat. Rev. Drug Discov.*, 5(9):730–739, 2006. doi: 10.1038/nrd2082.

[2] D. C. Swinney. Biochemical mechanisms of drug action: what does it take for success? *Nat. Rev. Drug Discov.*, 3(9):801–808, 2004. doi: 10.1038/nrd1500.

[3] P. J. Tummino and R. A. Copeland. Residence time of receptor-ligand complexes and its effect on biological function. *Biochemistry*, 47(20):5481–5492, 2008. doi: 10.1021/bi8002023.

[4] S. Núñez, J. Venhorst, and C. G. Kruse. Target-drug interactions: first principles and their application to drug discovery. *Drug Discov. Today*, 17(1-2):10–22, 2012. doi: 10.1016/j.drudis.2011.06.013.

[5] P. Ehrlich. Chemotherapeutics: scientific principles, methods and results. *Lancet*, 182(4694):445–451, 1913.

[6] R. A. Copeland. The drug-target residence time model: a 10-year retrospective. *Nat. Rev. Drug Discov.*, 15(2):87–95, 2016. doi: 10.1038/nrd.2015.18.

[7] R. A. Copeland. Conformational adaptation in drug-target interactions and residence time. *Future Med. Chem.*, 3(12):1491–1501, 2011. doi: 10.4155/fmc.11.112.

[8] J. M. Bradshaw, J. M. McFarland, V. O. Paavilainen, A. Bisconte, D. Tam, V. T. Phan, S. Romanov, D. Finkle, J. Shu, V. Patel, T. Ton, X. Li, D. G. Loughhead, P. A. Nunn, D. E. Karr, M. E. Gerritsen, J. O. Funk, T. D. Owens, E. Verner, K. A. Brameld, R. J. Hill, D. M. Goldstein, and J. Taunton. Prolonged and tunable residence time using reversible covalent kinase inhibitors. *Nat. Chem. Biol.*, 11 (7):525–531, 2015. doi: 10.1038/nchembio.1817.

[9] G. K. Walkup, Z. You, P. L. Ross, E. K. H. Allen, F. Daryaee, M. R. Hale, J. O'Donnell, D. E. Ehmann, V. J. A. Schuck, E. T. Buurman, A. L. Choy, L. Hajec, K. Murphy-Benenato, V. Marone, S. A. Patey, L. A. Grosser, M. Johnstone, S. G. Walker, P. J. Tonge, and S. L. Fisher. Translating slow-binding inhibition kinetics into cellular and in vivo effects. *Nat. Chem. Biol.*, 11(6):416–423, 2015. doi: 10.1038/nchembio.1796.

[10] S. Davoodi, F. Daryaee, A. Chang, S. G. Walker, and P. J. Tonge. Correlating drug-target residence time and post-antibiotic effect: Insight into target vulnerability. *ACS Infect. Dis.*, 6(4):629–636, 2020. doi: 10.1021/acsinfecdis.9b00484.

[11] G. Vauquelin. Effects of target binding kinetics on in vivo drug efficacy: k_{off}, k_{on} and rebinding. *Br. J. Pharmacol.*, 173(15):2319–2334, 2016. doi: 10.1111/bph.13504.

[12] R. H. A. Folmer. Drug target residence time: a misleading concept. *Drug Discov. Today*, 23(1):12–16, 2018. doi: 10.1016/j.drudis.2017.07.016.

[13] T. M. Apostol. *Mathematical Analysis*. Addison-Wesley, Reading, MA, 2nd edition, 1974.

[14] P. Csermely, R. Palotai, and R. Nussinov. Induced fit, conformational selection and independent dynamic segments: an extended view of binding events. *Trends Biochem. Sci.*, 35(10):539–546, 2010. doi: 10.1016/j.tibs.2010.04.009.

[15] A. D. Vogt and E. Di Cera. Conformational selection or induced fit? A critical appraisal of the kinetic mechanism. *Biochemistry*, 53(36):5723–5729, 2014. doi: 10.1021/bi500913n.

[16] R. A. Copeland. Evolution of the drug-target residence time model. *Expert Opin. Drug Discov.*, 16(12): 1441–1451, 2021. doi: 10.1080/17460441.2021.1948997.

[17] W. Walter. *Ordinary Differential Equations*. Springer-Verlag, New York, 1998. doi: 10.1007/978-1-4612-0601-9.

Appendices

A Alternative exponential bounds via variation of constants

In Section 4, we derived bounds on EOT_∞ using comparison with constant-coefficient linear equations. Here we present an alternative approach using variation of constants, which yields bounds with exponential correction factors. These bounds can be sharper in certain parameter regimes.

A.1 Setup

Recall from equation (49) that the complex concentration satisfies:

$$\dot{c} = -[k_1 b_0 \exp(-k_3 t) + k_2]c + k_1 a_0 b_0 \exp(-k_3 t), \qquad c(0) = 0. \tag{65}$$

The homogeneous equation $\dot{v} = -[k_1 b_0 \exp(-k_3 t) + k_2]v$ has solution:

$$v(t) = \exp\left(-\int_0^t [k_1 b_0 \exp(-k_3 s) + k_2]\,\mathrm{d}s\right). \tag{66}$$

Evaluating the integral:

$$\begin{aligned}\int_0^t [k_1 b_0 \exp(-k_3 s) + k_2]\,\mathrm{d}s &= k_1 b_0 \int_0^t \exp(-k_3 s)\,\mathrm{d}s + k_2 t \\ &= \frac{k_1 b_0}{k_3}[1 - \exp(-k_3 t)] + k_2 t.\end{aligned} \tag{67}$$

Therefore:

$$v(t) = \exp\left(\frac{k_1 b_0}{k_3}[\exp(-k_3 t) - 1] - k_2 t\right). \tag{68}$$

This can be rewritten as:

$$v(t) = \exp\left(-\frac{k_1 b_0}{k_3}\right)\exp\left(\frac{k_1 b_0}{k_3}\exp(-k_3 t)\right)\exp(-k_2 t). \tag{69}$$

A.2 Bounds on the Homogeneous Solution

For $t \geq 0$, we have $0 \leq \exp(-k_3 t) \leq 1$, which implies:

$$0 \leq \frac{k_1 b_0}{k_3}\exp(-k_3 t) \leq \frac{k_1 b_0}{k_3}.$$

Since the exponential function is monotonically increasing:

$$1 \leq \exp\left(\frac{k_1 b_0}{k_3}\exp(-k_3 t)\right) \leq \exp\left(\frac{k_1 b_0}{k_3}\right).$$

Substituting into (69):

$$\exp\left(-\frac{k_1 b_0}{k_3}\right)\exp(-k_2 t) \leq v(t) \leq \exp(-k_2 t). \tag{70}$$

For the inverse:

$$\exp(k_2 t) \leq v(t)^{-1} \leq \exp\left(\frac{k_1 b_0}{k_3}\right)\exp(k_2 t). \tag{71}$$

A.3 Solution via Variation of Constants

The solution to (65) can be written as $c(t) = w(t)v(t)$, where $w(t)$ satisfies:

$$\dot{w}(t) = k_1 a_0 b_0 \exp(-k_3 t) \cdot v(t)^{-1}, \qquad w(0) = 0. \tag{72}$$

Upper Bound on $w(t)$. Using the upper bound from (71):

$$\dot{w}(t) \leq k_1 a_0 b_0 \exp\left(\frac{k_1 b_0}{k_3}\right) \exp((k_2 - k_3)t).$$

Integrating from 0 to t (for $k_2 \neq k_3$):

$$w(t) \leq \frac{k_1 a_0 b_0}{k_2 - k_3} \exp\left(\frac{k_1 b_0}{k_3}\right) [\exp((k_2 - k_3)t) - 1]. \tag{73}$$

Lower Bound on $w(t)$. Using the lower bound from (71):

$$\dot{w}(t) \geq k_1 a_0 b_0 \exp((k_2 - k_3)t).$$

Integrating:

$$w(t) \geq \frac{k_1 a_0 b_0}{k_2 - k_3} [\exp((k_2 - k_3)t) - 1]. \tag{74}$$

A.4 Bounds on $c(t)$

Combining the bounds on $w(t)$ and $v(t)$:

Upper Bound. Using (73) and the upper bound on $v(t)$ from (70):

$$\begin{aligned} c(t) = w(t)v(t) &\leq \frac{k_1 a_0 b_0}{k_2 - k_3} \exp\left(\frac{k_1 b_0}{k_3}\right) [\exp((k_2 - k_3)t) - 1] \cdot \exp(-k_2 t) \\ &= \frac{k_1 a_0 b_0}{k_2 - k_3} \exp\left(\frac{k_1 b_0}{k_3}\right) [\exp(-k_3 t) - \exp(-k_2 t)]. \end{aligned} \tag{75}$$

Lower Bound. Using (74) and the lower bound on $v(t)$ from (70):

$$\begin{aligned} c(t) &\geq \frac{k_1 a_0 b_0}{k_2 - k_3} [\exp((k_2 - k_3)t) - 1] \cdot \exp\left(-\frac{k_1 b_0}{k_3}\right) \exp(-k_2 t) \\ &= \frac{k_1 a_0 b_0}{k_2 - k_3} \exp\left(-\frac{k_1 b_0}{k_3}\right) [\exp(-k_3 t) - \exp(-k_2 t)]. \end{aligned} \tag{76}$$

A.5 Bounds on EOT_∞

Integrating (75) and (76) over $[0, \infty)$ and dividing by a_0 yields the exponential bounds.

Upper bound.

$$\begin{aligned}\mathrm{EOT}_\infty &\le \frac{k_1 b_0}{k_2 - k_3} \exp\left(\frac{k_1 b_0}{k_3}\right) \int_0^\infty [\exp(-k_3 t) - \exp(-k_2 t)]\,\mathrm{d}t \\ &= \frac{k_1 b_0}{k_2 - k_3} \exp\left(\frac{k_1 b_0}{k_3}\right) \cdot \frac{k_2 - k_3}{k_2 k_3} \\ &= \exp\left(\frac{k_1 b_0}{k_3}\right) \frac{b_0}{K_d k_3}. \end{aligned} \tag{77}$$

Lower bound.

$$\begin{aligned}\mathrm{EOT}_\infty &\ge \exp\left(-\frac{k_1 b_0}{k_3}\right) \frac{k_1 b_0}{k_2 k_3} \\ &= \exp\left(-\frac{k_1 b_0}{k_3}\right) \frac{b_0}{K_d k_3}. \end{aligned} \tag{78}$$

Combining these results:

$$\boxed{\exp\left(-\frac{k_1 b_0}{k_3}\right) \frac{b_0}{K_d k_3} \le \mathrm{EOT}_\infty \le \exp\left(\frac{k_1 b_0}{k_3}\right) \frac{b_0}{K_d k_3}} \tag{79}$$

A.6 Comparison with Standard Bounds

In Section 4, we derived the standard bounds:

$$\frac{b_0}{(b_0 + K_d)k_3} \le \mathrm{EOT}_\infty \le \frac{b_0}{K_d k_3}.$$

Upper bounds. The standard upper bound is $b_0/(K_d k_3)$, while the exponential upper bound is $\exp(k_1 b_0/k_3) \cdot b_0/(K_d k_3)$. Since $\exp(k_1 b_0/k_3) \ge 1$, the **standard upper bound is always tighter**.

Lower bounds. The standard lower bound is $b_0/[(b_0 + K_d)k_3]$, while the exponential lower bound is $\exp(-k_1 b_0/k_3) \cdot b_0/(K_d k_3)$. The standard lower bound is tighter when:

$$\frac{b_0}{(b_0 + K_d)k_3} \ge \exp\left(-\frac{k_1 b_0}{k_3}\right) \frac{b_0}{K_d k_3},$$

which simplifies to:

$$\frac{K_d}{b_0 + K_d} \ge \exp\left(-\frac{k_1 b_0}{k_3}\right),$$

or equivalently:

$$1 + \frac{b_0}{K_d} \le \exp\left(\frac{k_1 b_0}{k_3}\right).$$

Using the inequality $1+x \le \exp(x)$ for all $x \ge 0$, this condition is satisfied whenever $b_0/K_d \le (b_0/K_d)\cdot(k_2/k_3)$, which holds when $k_2 \ge k_3$—that is, when dissociation is at least as fast as elimination. Since this is the biologically common regime, the **standard lower bound is typically tighter**.

Remark 6. *The exponential bounds may be useful in specialized scenarios where $k_3 > k_2$ (elimination faster than dissociation) or when asymptotic analysis is required. For most practical applications, the standard bounds from Section 4 are preferred.*

B Practical Guide to EOT Measurement and Application

This appendix provides experimental protocols and practical guidance for measuring the parameters required to apply the EOT framework, validating predictions experimentally, and using EOT to guide drug optimization.

B.1 Parameter Estimation

Applying the EOT framework requires accurate measurement of the association rate constant k_1, dissociation rate constant k_2, and elimination rate constant k_3.

B.1.1 Measuring k_1 and k_2 (Biochemical)

Surface Plasmon Resonance (SPR). Purified target protein is immobilized on a sensor chip, and drug solutions are flowed across the surface at 5–7 concentrations spanning $0.1K_d$ to $10K_d$. The association phase (drug flow ON) and dissociation phase (drug flow OFF) are recorded, and the resulting sensorgrams are fit globally to a 1:1 Langmuir binding model:

$$R(t) = R_{\max}[1 - \exp(-(k_1 C + k_2)t)] \quad \text{(association)}$$
$$R(t) = R_0 \exp(-k_2 t) \quad \text{(dissociation)}$$

Modern instruments provide k_1 accurate to within 20–30% and k_2 to within 10–20%.

Bio-Layer Interferometry (BLI). BLI operates on a similar principle to SPR but uses fiber-optic sensors. Its advantages include simpler operation without microfluidics, real-time analysis capability, and suitability for crude lysates. However, BLI has lower sensitivity than SPR for very tight binders ($K_d < 1$ nM).

Stopped-Flow Fluorescence. For very fast kinetics ($k_1 > 10^7$ $\mathrm{M^{-1}s^{-1}}$, $k_2 > 10$ $\mathrm{s^{-1}}$) that exceed SPR temporal resolution, stopped-flow fluorescence provides an alternative. This technique requires a fluorescent drug or labeled target, and the mixing dead-time of approximately 1 ms limits measurements to systems where $k_1 b_0 + k_2 < 1000$ $\mathrm{s^{-1}}$.

Quality Control. The kinetically determined dissociation constant $K_d^{\text{kinetic}} = k_2/k_1$ should agree with the equilibrium value K_d^{eq} from dose-response curves within 2–3 fold. Large discrepancies suggest non-1:1 binding stoichiometry, mass transport artifacts in SPR, or heterogeneous protein preparation.

B.1.2 Measuring Cellular k_1^{cell} and k_2^{cell}

Cellular rate constants often differ from biochemical values due to molecular crowding (approximately 30% of cytoplasmic volume is occupied by macromolecules, reducing effective diffusion), subcellular localization requiring drugs to traverse membranes, and competition from endogenous ligands.

Washout Experiments. Cells are treated with drug to achieve equilibrium, then extracellular drug is removed by rapid media exchange. Intracellular target occupancy is monitored over time using fluorescent drugs with confocal microscopy, NanoBRET target engagement assays, or cellular thermal shift assay (CETSA). The decay of the occupancy signal is fit to an exponential to extract k_2^{cell}.

Pulse-Chase with Competition. A saturating concentration of unlabeled competitor is added after equilibration with labeled drug. The rate of displacement yields k_2^{cell}, provided the competitor concentration greatly exceeds K_d so that dissociation is rate-limiting.

Measuring k_1^{cell}. Measuring the cellular association rate is more challenging than measuring k_2^{cell}. Two approaches are available: measuring the association time-course at multiple drug concentrations and fitting to the integrated rate equation, or calculating $k_1^{\text{cell}} = k_2^{\text{cell}}/K_d^{\text{cell}}$ if the cellular dissociation constant is independently measurable.

B.1.3 Measuring k_3

In Vitro: Liver Microsome Stability. Incubate drug (1 μM) with pooled liver microsomes (0.5 mg/mL protein, species-matched). Sample at 0, 5, 15, 30, 60 min. Quantify remaining drug by LC-MS/MS. Fit to exponential decay: $[\text{drug}](t) = [\text{drug}]_0 \exp(-k_3^{\text{mic}} t)$. This measures hepatic metabolism (CYP450, UGT, etc.) but omits renal excretion and extrahepatic metabolism.

Hepatocyte Stability. Similar protocol using cryopreserved hepatocytes. More physiological (intact cellular transporters, cofactors) but higher variability. Typical k_3 values: stable drugs < 0.01 min^{-1} (long half-life), labile drugs > 0.1 min^{-1} (short half-life).

In Vivo Pharmacokinetics. Administer single IV dose to animals (mice, rats). Collect plasma at 0.08, 0.25, 0.5, 1, 2, 4, 8, 24 h. Fit concentration-time profile to exponential or multi-exponential model. For simple one-compartment kinetics, elimination rate $k_3 = \text{clearance}/V_d$ where V_d is volume of distribution.

Intracellular k_3. Critical for intracellular targets. Measure intracellular drug concentration (cell lysis + LC-MS or using fluorescent drugs + flow cytometry) following washout. Cellular k_3 includes: active efflux (P-gp, BCRP), passive diffusion, and intracellular metabolism. Can differ dramatically from plasma k_3.

Example 6. *Some kinase inhibitors have plasma $t_{1/2} \sim 10$ h but intracellular $t_{1/2} \sim 2$ h due to MDR1 efflux.*

Table 5 summarizes typical ranges for these kinetic parameters encountered in drug discovery.

Table 5: Typical ranges for kinetic and elimination parameters in drug-target binding.

Parameter	Typical Range
k_1	10^4 to 10^7 M^{-1}s^{-1} (diffusion-limited upper bound $\sim 10^9$)
k_2	10^{-4} to 1 s^{-1} (ultra-tight binders to weak binders)
k_3	10^{-5} to 1 s^{-1} (stable drugs to rapidly cleared drugs)

B.2 Calculating Predicted EOT

With measured parameters, compute predictions using the results from the main text.

B.2.1 Closed Systems (In Vitro Assays)

Use equation (24):

$$\text{rEOT} \approx f_\infty = \frac{b_0}{K_d + b_0}.$$

Example 7. *If assay time $T = 2$ h with $b_0 = 1$ μM, $K_d = 0.1$ μM:*

$$\text{rEOT} \approx \frac{1}{0.1 + 1} = 0.91,$$

so $\text{EOT}(2\,\text{h}) \approx 0.91 \times 2 = 1.82$ *h. Interpretation: On average, each receptor spends 1.82 of the 2-hour period bound to drug.*

B.2.2 Open Systems (With Drug Elimination)

Use the bounds from equation (61):

$$\frac{b_0}{(b_0 + K_d)k_3} \leq \text{EOT}_\infty \leq \frac{b_0}{K_d \cdot k_3}.$$

Example 8. *If $k_1^{\text{cell}} = 10^6$ $M^{-1}s^{-1}$, $k_2^{\text{cell}} = 0.01$ s^{-1}, $k_3^{\text{cell}} = 0.001$ s^{-1} (slow efflux), $b_0 = 1$ μM:*

$$K_d = \frac{0.01}{10^6} = 10^{-8}\,\text{M} = 0.01\,\mu\text{M}.$$

$$\frac{1}{(1 + 0.01) \times 0.001} \leq \text{EOT}_\infty \leq \frac{1}{0.01 \times 0.001}$$

$$990\,\text{s} \leq \text{EOT}_\infty \leq 100{,}000\,\text{s}.$$

Even the lower bound predicts ∼16 minutes of cumulative occupancy, explaining prolonged cellular effects after washout.

B.2.3 Induced Fit Systems

Use equation (42) with effective dissociation constant $K_d^* = K_d/(1 + k_3/k_4)$:

$$f_\infty = \frac{b_0}{K_d^* + b_0}.$$

Example 9. *If $K_d = 1$ μM and $k_3/k_4 = 9$ (strong induced fit), then $K_d^* = 0.1$ μM. At $b_0 = 1$ μM:*

$$f_\infty = \frac{1}{0.1 + 1} = 0.91,$$

compared to $f_\infty = 0.5$ without induced fit. The conformational trapping nearly doubles target occupancy.

B.3 Testable Predictions

The EOT framework generates specific, experimentally testable predictions that distinguish it from simpler models.

B.3.1 Prediction 1: Concentration-Dependence of Residence Time

Copeland DTRT predicts that residence time is independent of drug concentration. In contrast, our equation (61) predicts concentration-dependent behavior: at low drug concentration ($b_0 \ll K_d$), $\text{EOT}_\infty \approx (k_1 b_0)/(k_2 k_3)$, scaling linearly with concentration, while at high drug concentration ($b_0 \gg K_d$), $\text{EOT}_\infty \approx 1/k_3$, becoming independent of concentration.

Experimental test. Measure target occupancy time (e.g., using washout experiments or cellular target engagement assays) across a range of drug concentrations in systems with known k_3. The transition from linear to plateau behavior should occur near $b_0 \approx K_d$. FIGURE 4 illustrates this predicted behavior for three different elimination rates.

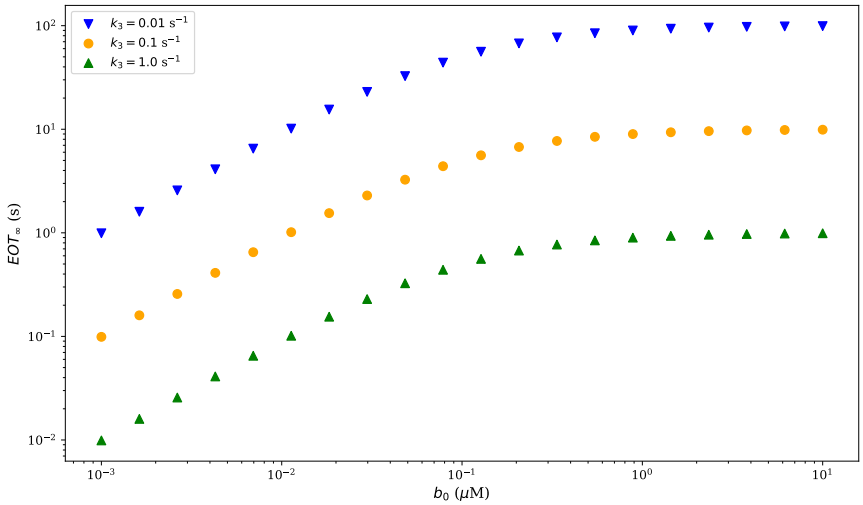

Figure 4: **Predicted concentration-dependence of** EOT_∞**.** EOT_∞ varies with drug concentration b_0 for different elimination rates k_3. At low concentrations ($b_0 \ll K_d$), EOT_∞ scales linearly with b_0. At high concentrations ($b_0 \gg K_d$), EOT_∞ plateaus at $1/k_3$. The transition occurs near $b_0 = K_d$. Different curves show systems with $k_3 = 0.01$ s^{-1} (blue, downward triangles), $k_3 = 0.1$ s^{-1} (orange, circles), and $k_3 = 1.0$ s^{-1} (green, upward triangles). Parameters: $k_1 = 10^6$ M^{-1}s^{-1}, $k_2 = 0.1$ s^{-1} ($K_d = 0.1$ μM).

Detailed protocol. Begin by selecting a well-characterized drug-target pair with known k_1 and k_2 (e.g., dasatinib with Abl kinase). Prepare a cell-free system with purified components at varying drug concentrations spanning $0.1K_d$ to $10K_d$ (e.g., $0.1K_d$, $0.5K_d$, K_d, $2K_d$, $5K_d$, $10K_d$). At $t = 0$, mix components and measure fractional occupancy $f(t)$ at 10-minute intervals for 2 hours using fluorescence anisotropy (if the drug is fluorescent), competition binding with a radiolabeled tracer, or SPR if one component can be

immobilized. For each concentration, compute $\mathrm{EOT}(120\,\mathrm{min}) = \int_0^{120} f(t)\,\mathrm{d}t$ numerically via the trapezoidal rule, then plot $\mathrm{EOT}(120\,\mathrm{min})$ versus b_0. The expected behavior is a linear regime at low b_0, transitioning near $b_0 = K_d$ to a plateau approaching $120 \times b_0/(K_d + b_0)$ minutes at high b_0. Data should match equation (24) within experimental error (typically $\pm 15\%$).

B.3.2 Prediction 2: Effect of Elimination Rate

For a given drug with fixed k_1 and k_2 but varying k_3 (e.g., using metabolic inhibitors or comparing species with different clearance rates), EOT_∞ should scale as $1/k_3$ according to equation (61).

Experimental test. Compare target occupancy duration in wild-type versus metabolic enzyme knockout models, across species with different drug clearance rates (e.g., mouse vs. human), or in the presence versus absence of metabolic inhibitors such as CYP450 inhibitors. Our bounds predict the fold-change in EOT_∞ based on measured changes in k_3: if a CYP450 inhibitor reduces k_3 by 10-fold, EOT_∞ should increase by approximately 10-fold.

B.3.3 Prediction 3: Induced Fit Enhances Residence Time

Equation (42) predicts that drugs inducing conformational changes with large k_3/k_4 ratios achieve longer residence times than predicted from initial K_d alone.

Experimental test. For targets with known induced-fit mechanisms (e.g., kinases), first measure initial binding K_d using rapid equilibrium methods, then determine k_3 and k_4 using stopped-flow or temperature-jump kinetics. Use these parameters to predict rEOT via equation (42), and validate the prediction against measured target occupancy in cellular assays.

FIGURE 5 illustrates the predicted enhancement in fractional occupancy as a function of the k_3/k_4 ratio.

B.3.4 Prediction 4: Bounds Accuracy

Our analytical bounds (equations (61) and (79)) should bracket numerically computed EOT_∞ values across parameter space.

Experimental test. For drug-target pairs with measured k_1, k_2, k_3, compute the analytical bounds, measure actual occupancy time experimentally, and verify that experimental values fall within the predicted bounds.

Comprehensive numerical validation appears in FIGURES 2 and 3 in the main text.

B.4 Experimental Validation of EOT

B.4.1 Direct Target Occupancy Measurements

CETSA (Cellular Thermal Shift Assay). Drug binding stabilizes targets against thermal denaturation. In this assay, cells are treated with drug and optionally washed (if testing persistence of occupancy), then aliquots are heated to different temperatures (e.g., 40–65°C). After lysis, aggregated proteins are pelleted and the remaining soluble (non-aggregated) target is detected by Western blot. The shift in melting temperature (ΔT_m) correlates with fractional occupancy $f(t)$, and time-course CETSA post-washout directly measures how long targets remain occupied.

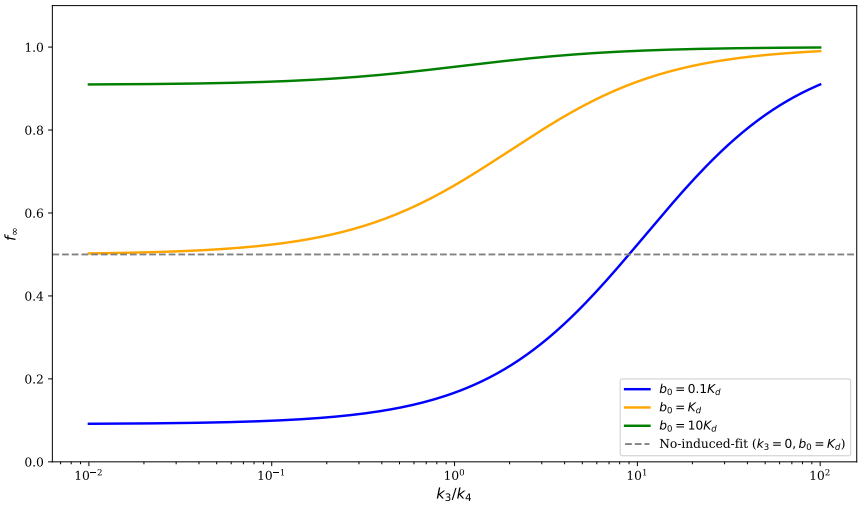

Figure 5: **Effect of induced fit on fractional occupancy f_∞.** Fractional occupancy vs. isomerization ratio k_3/k_4 for different drug concentrations. As k_3/k_4 increases (faster forward or slower reverse isomerization), the effective dissociation constant decreases ($K_d^* = K_d/(1 + k_3/k_4)$), increasing target occupancy. Blue: $b_0 = 0.1K_d$; orange: $b_0 = K_d$; green: $b_0 = 10K_d$. Dashed gray line shows the no-induced-fit case ($k_3 = 0$, $b_0 = K_d$). The effect is most pronounced at intermediate drug concentrations. Parameters: $K_d = 1$ μM.

NanoBRET Target Engagement. This approach requires engineering the target with a C-terminal NanoLuc tag. A membrane-permeable fluorescent tracer that binds the same site as the test drug is added, and drug binding displaces the tracer, reducing the BRET signal. This enables real-time measurement of intracellular occupancy in live cells, including association kinetics (monitoring BRET decrease upon drug addition), dissociation kinetics (monitoring BRET recovery after washout from equilibrium), and competition experiments with unlabeled compounds.

Quantitative Proteomics with Activity-Based Probes. For enzymes such as kinases and proteases, cells are pretreated with the test drug, washed, and then incubated with an active-site-directed covalent probe for a fixed labeling time. The amount of probe-labeled target is quantified by LC-MS/MS. Less labeled target indicates greater residual occupancy by the test drug, and a time course post-washout maps $f(t)$ directly.

B.4.2 Indirect Pharmacodynamic Readouts

When direct target occupancy is unmeasurable, use downstream biomarkers:

Kinase Inhibitors. Monitor substrate phosphorylation (e.g., ERK1/2 phosphorylation for MEK inhibitors). Assumption: phospho-signal proportional to fraction of active (unbound) kinase. Limitation: feedback loops complicate interpretation.

GPCR Antagonists. Pre-treat with antagonist, wash, stimulate with agonist at various times post-wash. Measure downstream response (cAMP, Ca^{2+} flux). Recovery of agonist response indicates antagonist disso-

ciation.

Antibiotics. Measure post-antibiotic effect (PAE): time required for bacteria to resume log-phase growth after antibiotic removal. PAE duration correlates with antibiotic-target occupancy time [10].

B.4.3 Integration of Experimental $f(t)$

Once $f(t)$ is measured at multiple time points, compute experimental EOT:

$$\mathrm{EOT}_{\mathrm{exp}}(T) = \int_0^T f_{\mathrm{exp}}(t)\,\mathrm{d}t \approx \sum_{i=1}^{N-1} \frac{f_{\mathrm{exp}}(t_i) + f_{\mathrm{exp}}(t_{i+1})}{2}(t_{i+1} - t_i) \tag{80}$$

using the trapezoidal rule. Compare with predicted $\mathrm{EOT}(T)$ from measured kinetic parameters.

B.4.4 Success Criteria

Good agreement (less than 2-fold difference between predicted and measured EOT) indicates the framework is validated for the system under study. Moderate discrepancy (2–5 fold) is likely due to parameter measurement errors (especially k_3), model simplifications such as ignoring target turnover, or cellular heterogeneity. Large discrepancy (greater than 5-fold) suggests additional complexity such as allosteric effects, multiple binding modes, active transport, or metabolism generating active metabolites.

B.5 Application to Drug Optimization

Use the validated framework to guide medicinal chemistry decisions.

If limited by binding kinetics ($k_3 \ll k_2$). Optimize structure to reduce k_2 (slower off-rate) by adding hydrogen bonds to deep pocket residues, increasing buried surface area, or inducing conformational traps that exploit the induced fit mechanism (Section 3). Monitor k_2 by SPR during structure-activity relationship (SAR) studies.

If limited by pharmacokinetics ($k_3 \gg k_2$). Two options are available. The first is to improve metabolic stability by blocking metabolic soft spots (e.g., reducing CYP3A4 turnover) or reducing efflux (avoiding P-gp substrates). The second is to accept short half-life and compensate by increasing dose or dosing frequency to maintain therapeutic $b(t)$.

Formulation strategies. When intrinsic k_2 cannot be improved, formulation approaches that effectively reduce k_3 can proportionally increase EOT_∞ (see equation (56)). Such approaches include sustained-release formulations, nanoparticle encapsulation, PEGylation for biologics, and depot injections.

B.6 Case Study Workflow

Hypothetical Kinase Inhibitor Program.

1. **Screening hit:** $K_d = 50$ nM (biochemical), cellular $\mathrm{IC}_{50} = 500$ nM.
2. **Measure kinetics:** $k_1 = 10^7\ \mathrm{M}^{-1}\mathrm{s}^{-1}$, $k_2 = 0.5\ \mathrm{s}^{-1}$ (SPR).

3. **Measure elimination:** $k_3^{\text{cell}} = 0.05\ \text{s}^{-1}$ (washout, $t_{1/2} = 14$ s).
4. **Predict EOT:** Using equation (56) at $b_0 = 500$ nM:

$$\text{EOT}_\infty^u = \frac{500\,\text{nM}}{50\,\text{nM} \times 0.05\,\text{s}^{-1}} = 200\,\text{s}.$$

5. **Diagnose problem:** Fast cellular elimination limits occupancy despite good K_d.
6. **Identify mechanism:** Caco-2 assay shows efflux ratio ER = 25 (P-gp substrate).
7. **Optimize:** Reduce basicity to avoid P-gp recognition.
8. **Result:** Next-generation compound has $k_3^{\text{cell}} = 0.005\ \text{s}^{-1}$ (10-fold improvement).
9. **Predicted improvement:** EOT_∞^u increases 10-fold to 2000 s.
10. **Validate:** CETSA confirms 10-fold longer target occupancy; cellular IC_{50} improves to 50 nM.

This workflow illustrates how the EOT framework connects binding kinetics, pharmacokinetics, and cellular efficacy into a unified optimization strategy.

B.7 Summary

The practical application of EOT centers on four interconnected activities. First, *measurement*: determining k_1 and k_2 (biochemically and/or in cells) along with the elimination rate k_3 in the relevant compartment. Second, *prediction*: calculating EOT or its bounds using the equations developed in the main text. Third, *validation*: comparing predicted EOT with experimentally measured target occupancy time courses to assess framework accuracy. Fourth, *optimization*: using the framework to identify whether binding kinetics or pharmacokinetics limits efficacy, and adjusting the optimization strategy accordingly. This systematic approach enables rational drug design that accounts for both target engagement and pharmacokinetic factors.